BEST AVAILABLE IMAGES

Defective images within this document are accurate representations of the original documents submitted by the applicant.

Defects in the images may include (but are not limited to):

- BLACK BORDERS
- TEXT CUT OFF AT TOP, BOTTOM OR SIDES
- FADED TEXT
- ILLEGIBLE TEXT
- SKEWED/SLANTED IMAGES
- COLORED PHOTOS
- BLACK OR VERY BLACK AND WHITE DARK PHOTOS
- GRAY SCALE DOCUMENTS

IMAGES ARE BEST AVAILABLE COPY.

As rescanning documents *will not* correct images, please do not report the images to the Image Problem Mailbox.

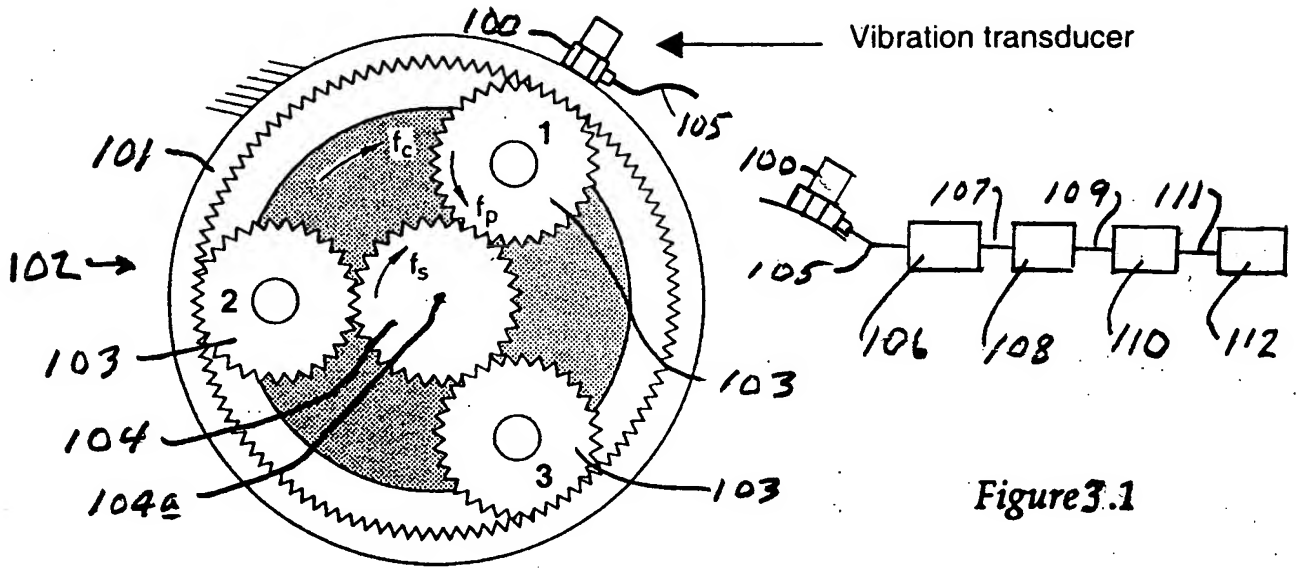

Figure 1.1: A three-planet epicyclic gear train with a fixed ring gear.

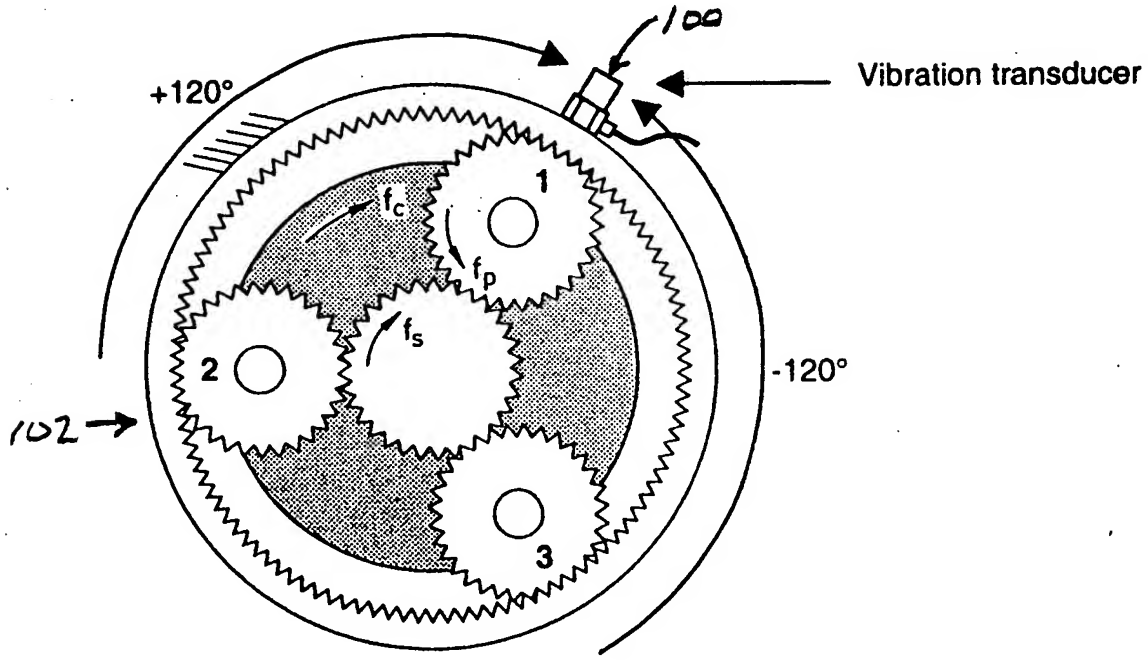

Figure 2.1: Phase shifts required to align the separated sun gear averages in a three-planet gear train.

a)

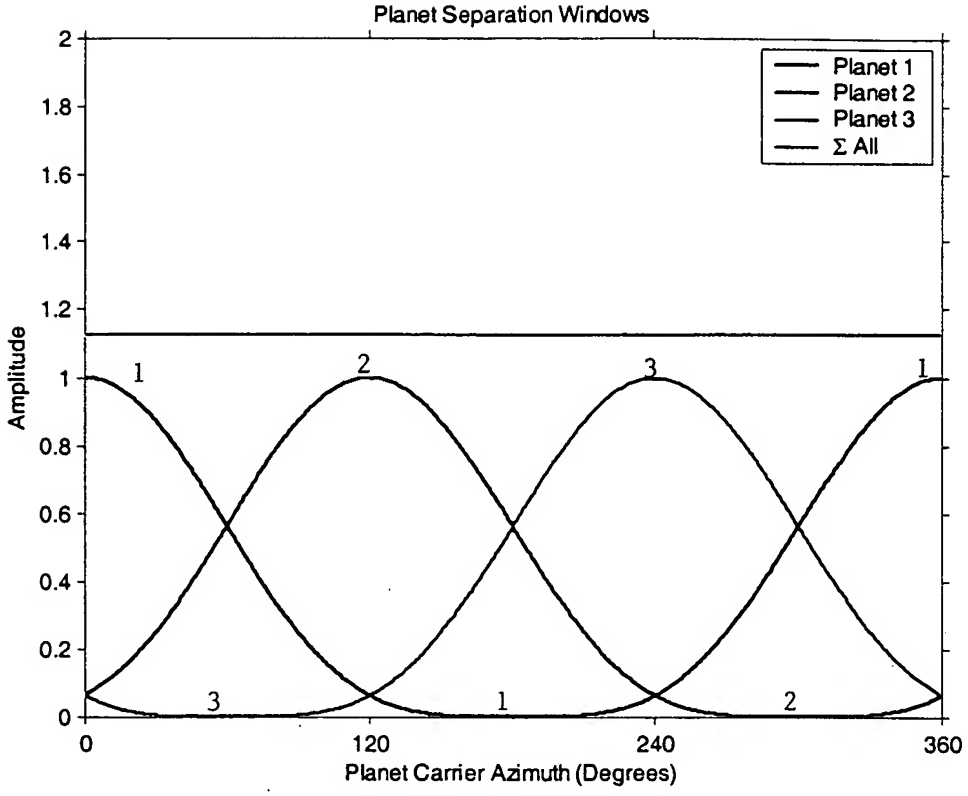

b)

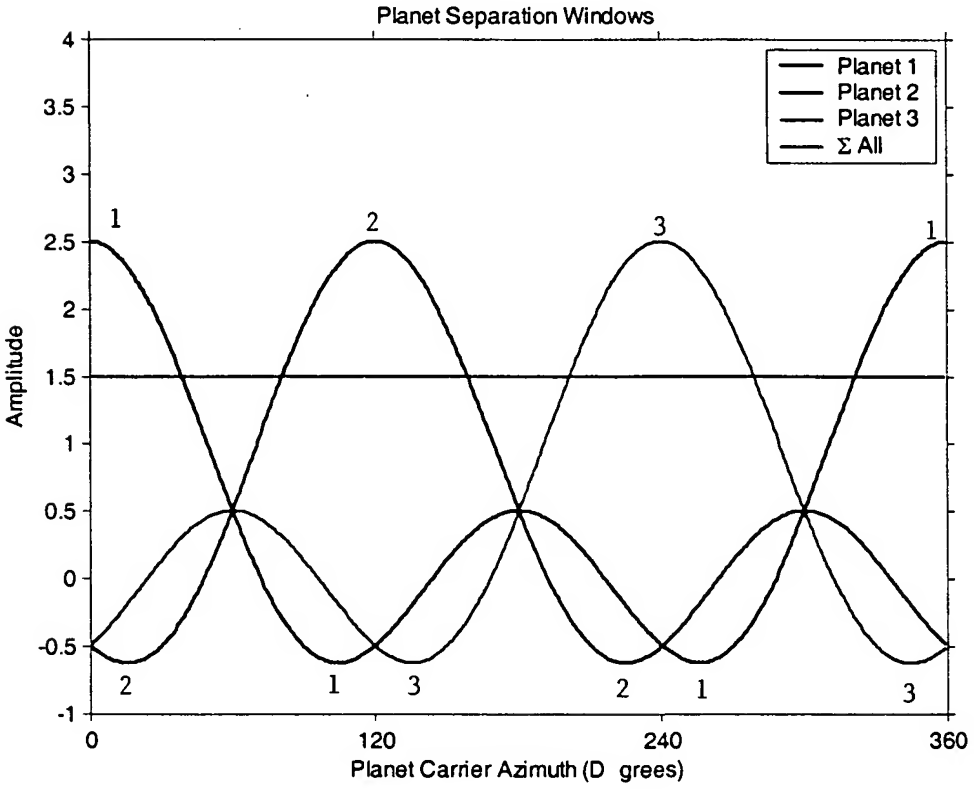

Figure 1.2: Separation window functions for a three-planet gear train: a) $w_{power}(t)$, b) $w_{sum}(t)$.

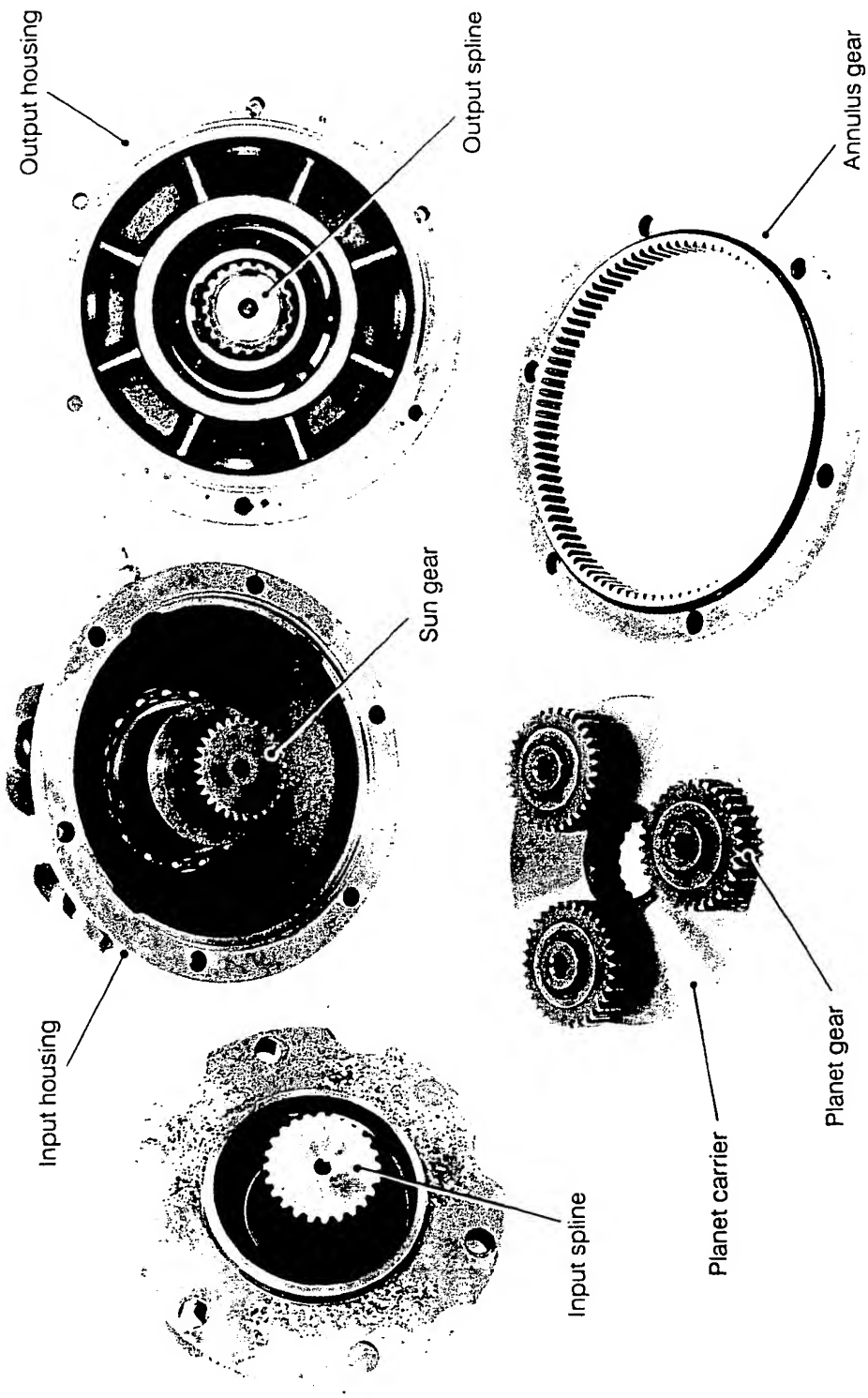

Figure 4.1: Exploded view of Brevini gearbox.

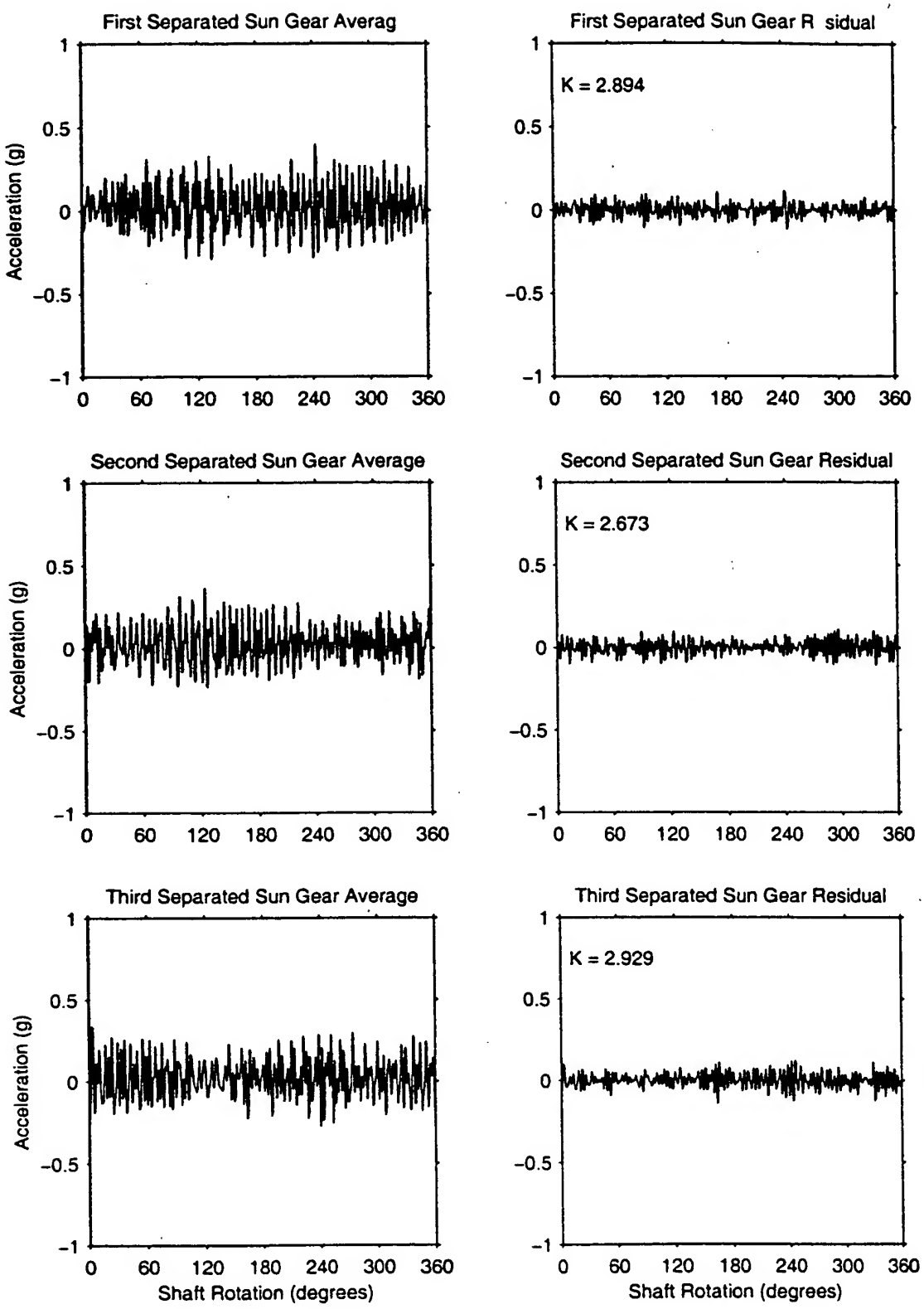

Figure 4.2: Sun gear separations (window = $w_{power}(t)$) – no fault.

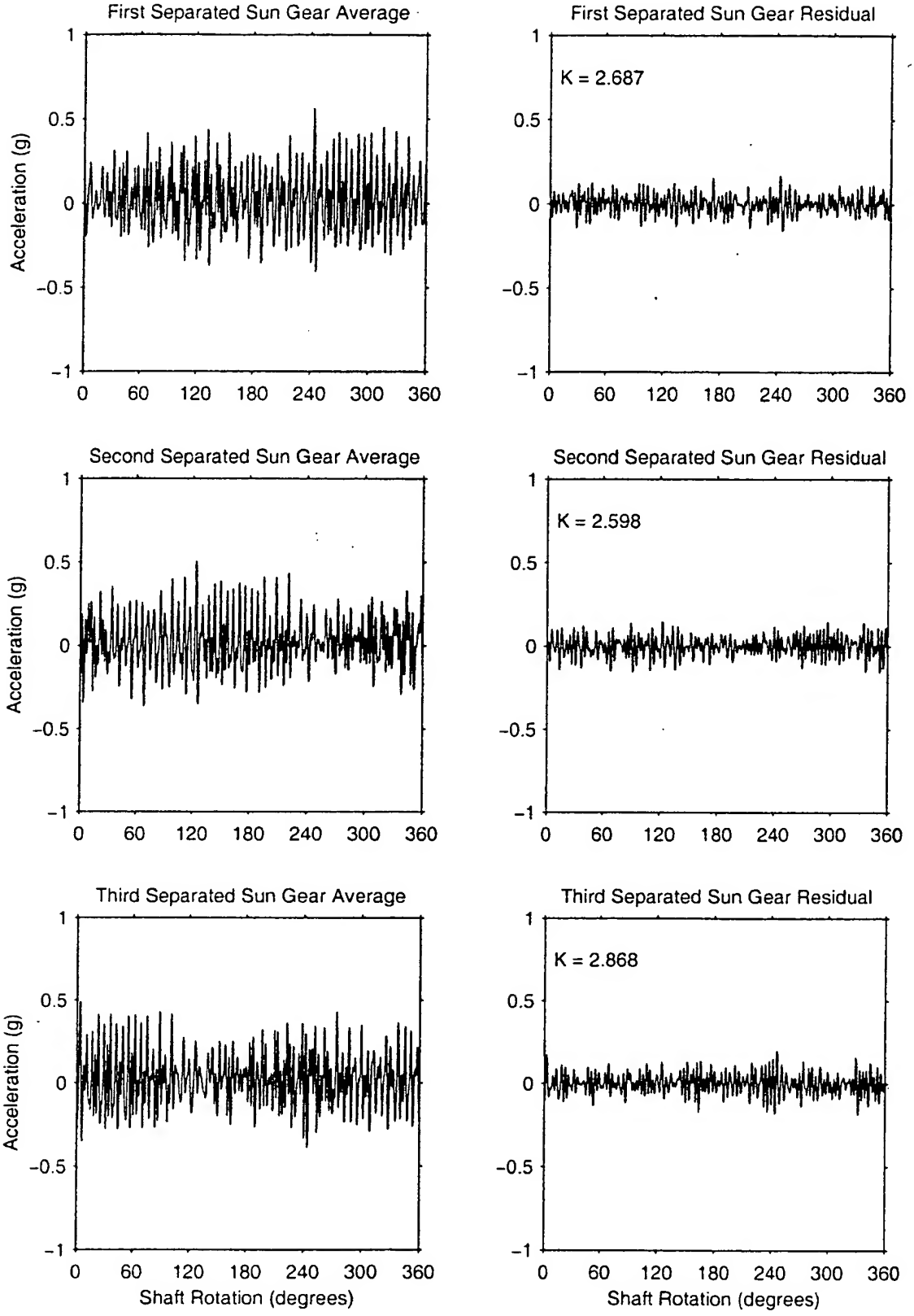

Figure 4.3: Sun gear separations (window = $w_{sum}(t)$) – no fault.

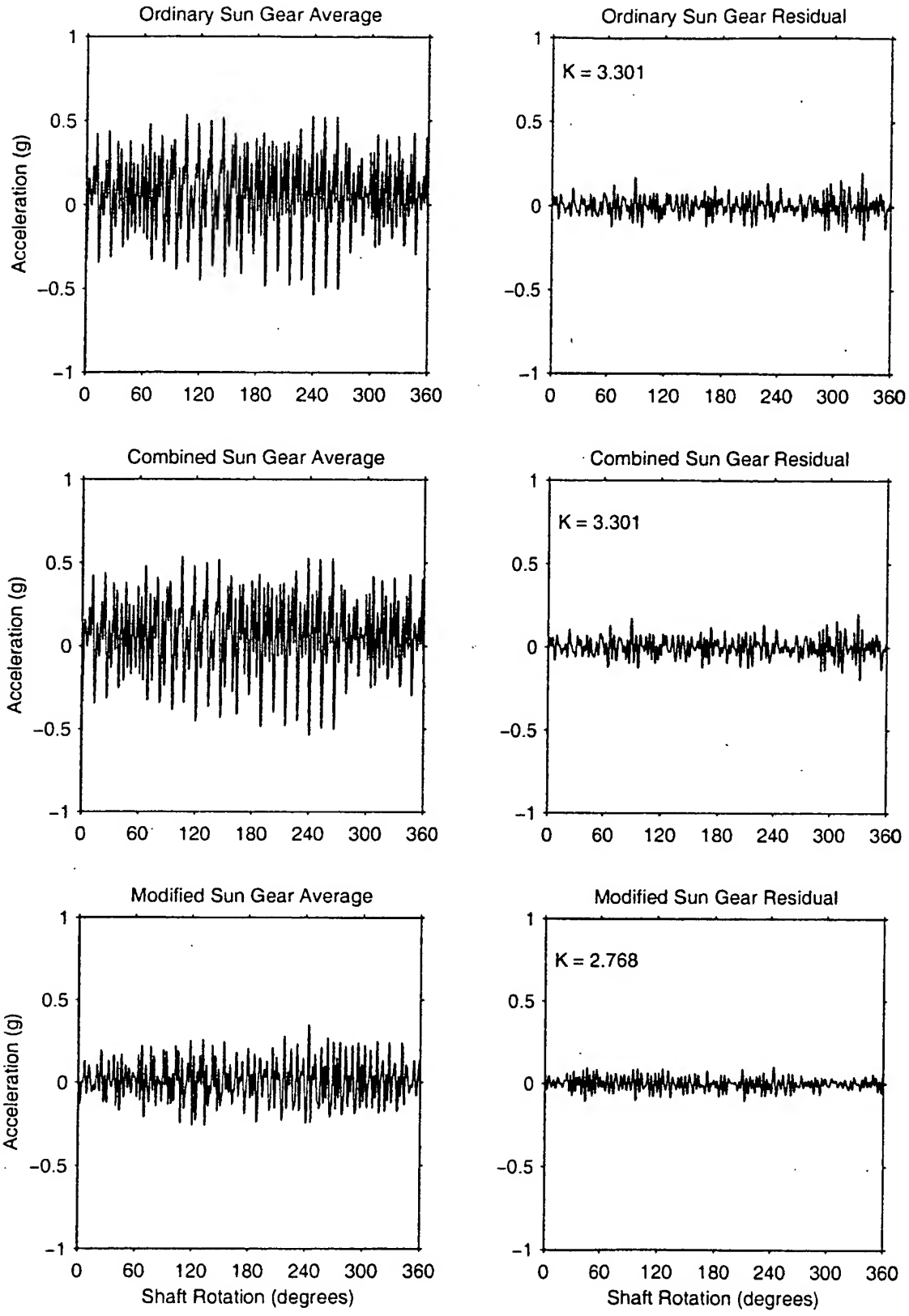

Figure 4.4: Ordinary, combined & modified sun gear averages (window = $w_{power}(t)$) – no fault.

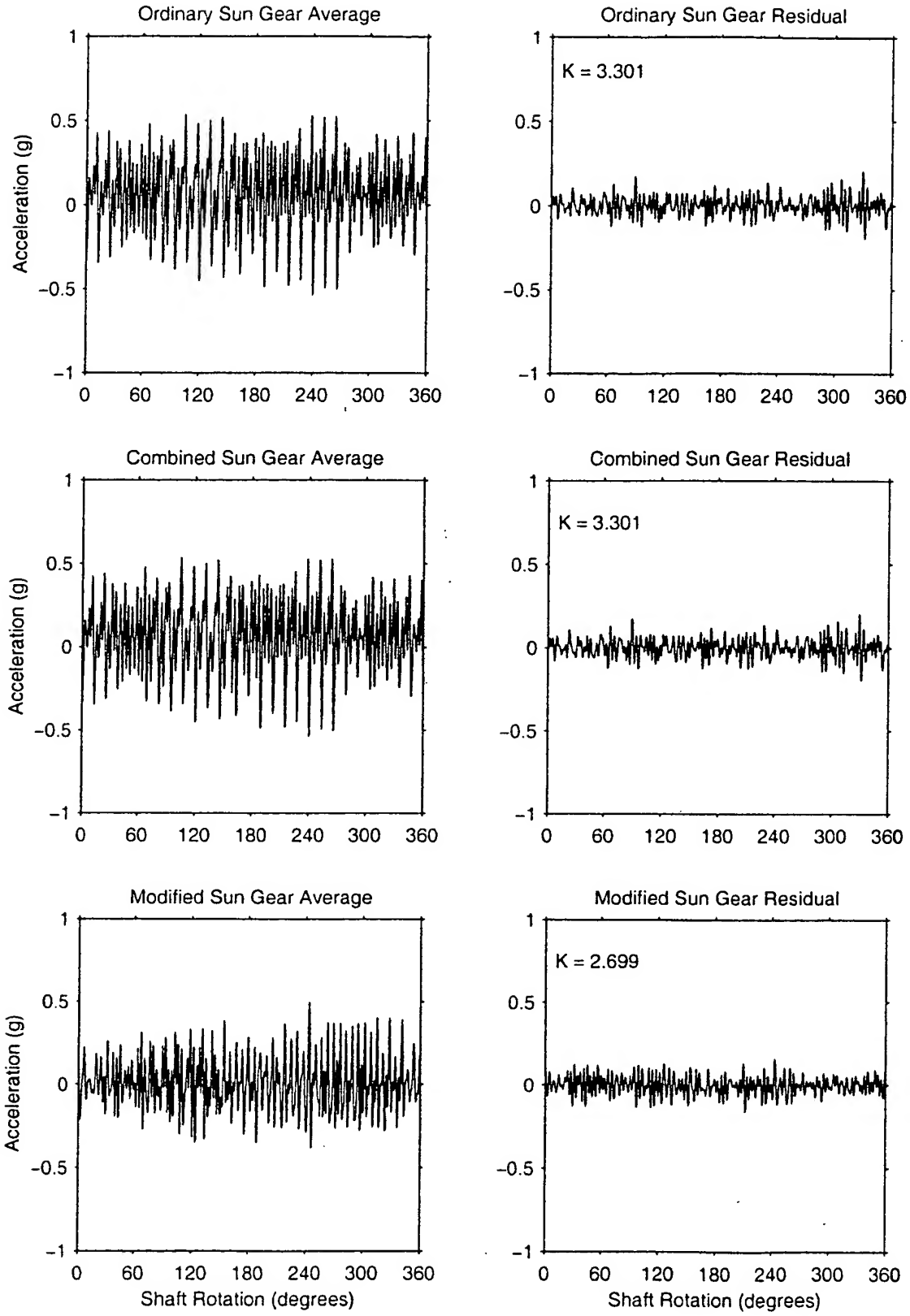

Figure 4.5. Ordinary, combined & modified sun gear averages (window = w.....(t)) – no fault.

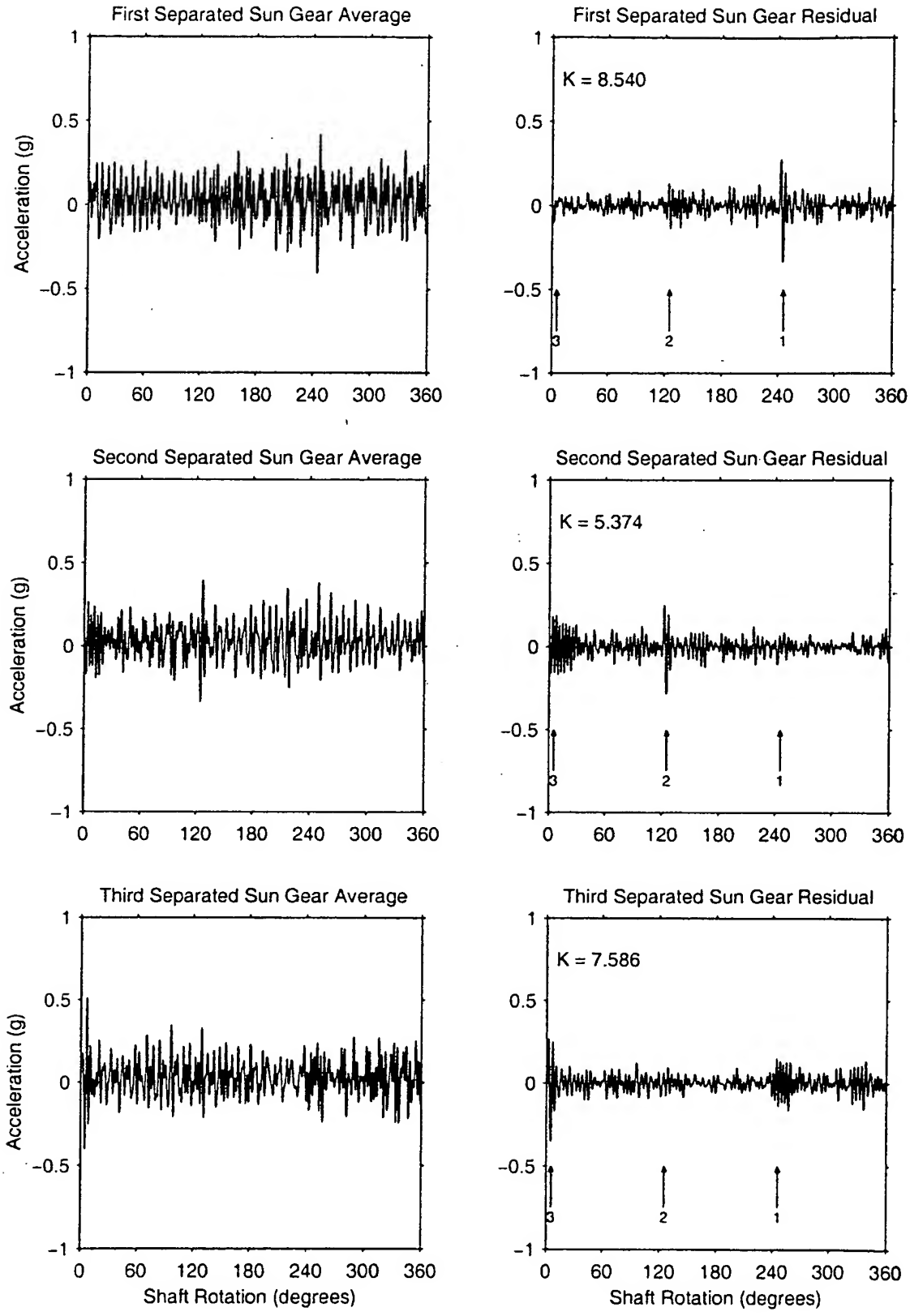

Figure 4.6: Sun gear separations (window = $w_{power}(t)$) – fault.

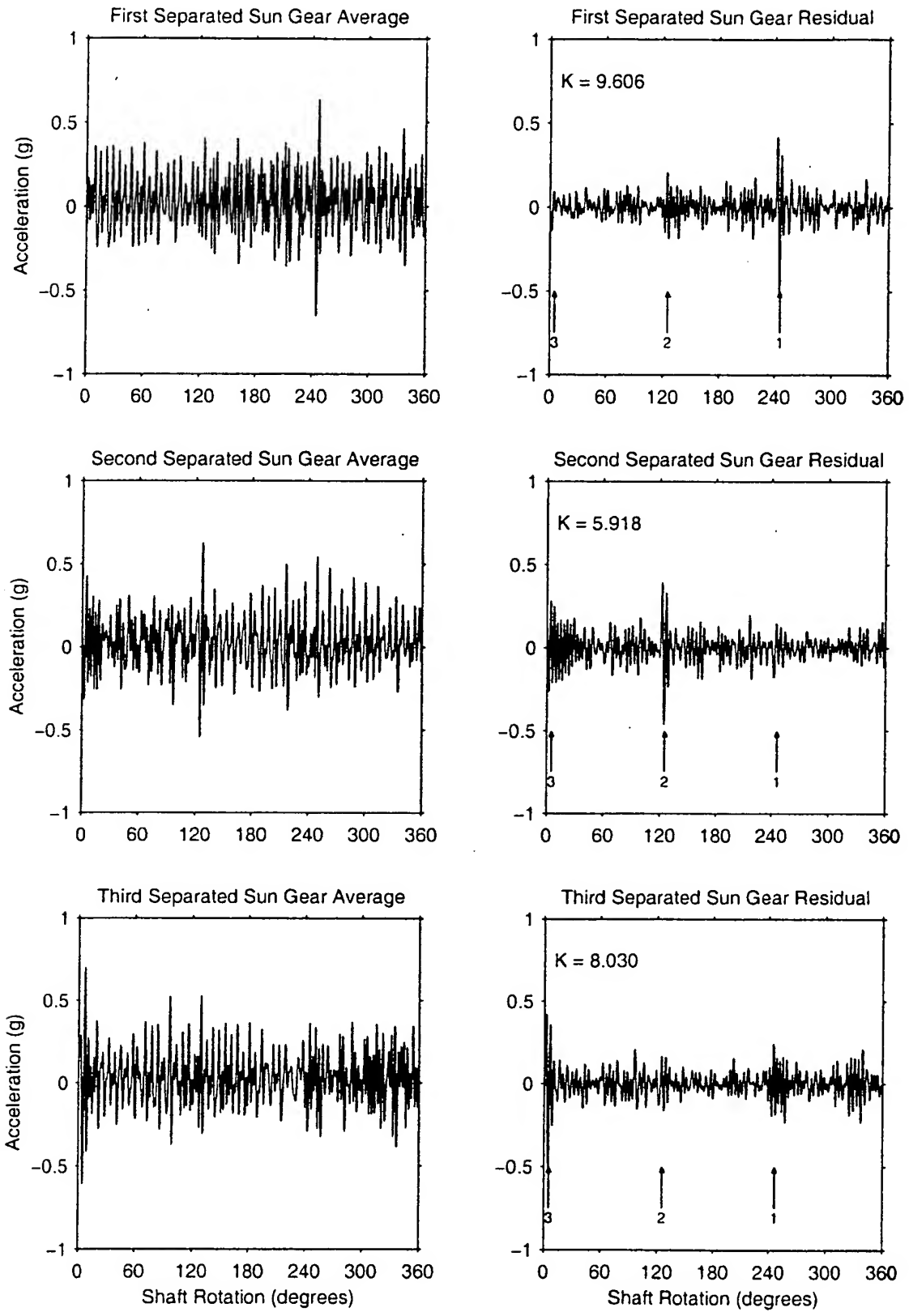

Figure 4.7: Sun gear separations (window = $w_{sum}(t)$) – fault.

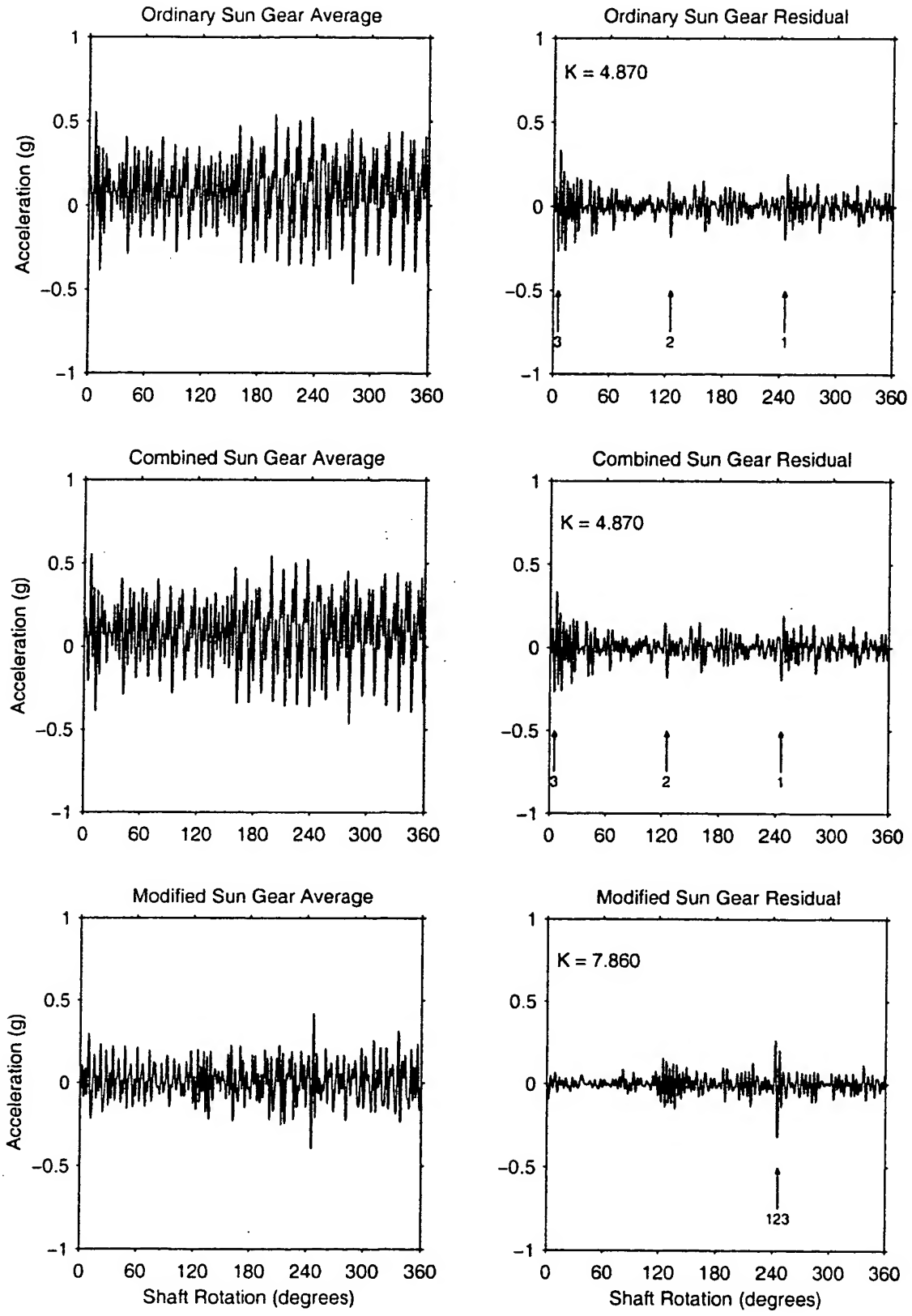

Figure 4.8: Ordinary, combined & modified sun gear averages (window = $w_{power}(t)$) – fault.

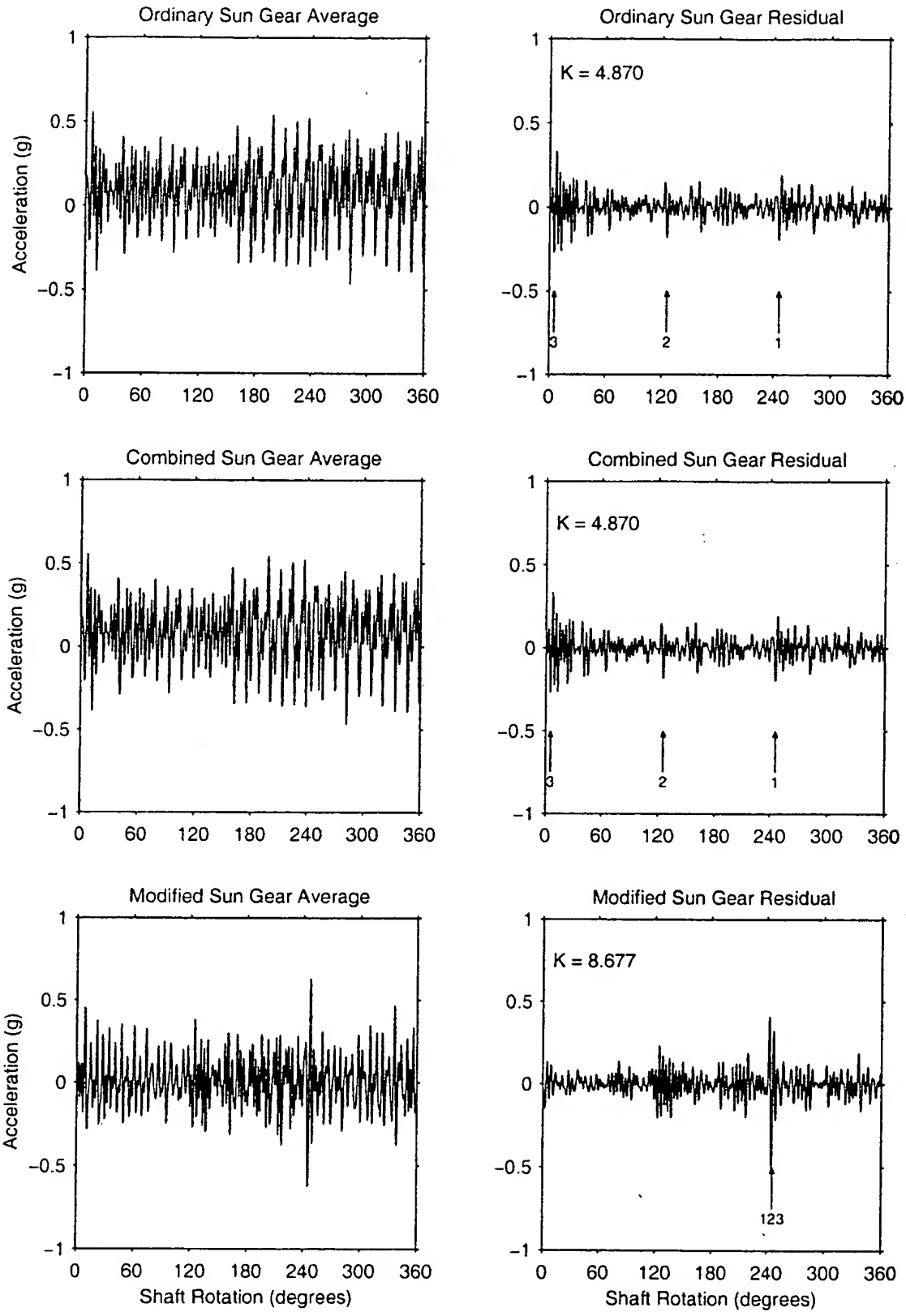

Figure 4.9: Ordinary, combined & modified sun gear averages (window = $w_{sum}(t)$) – fault.

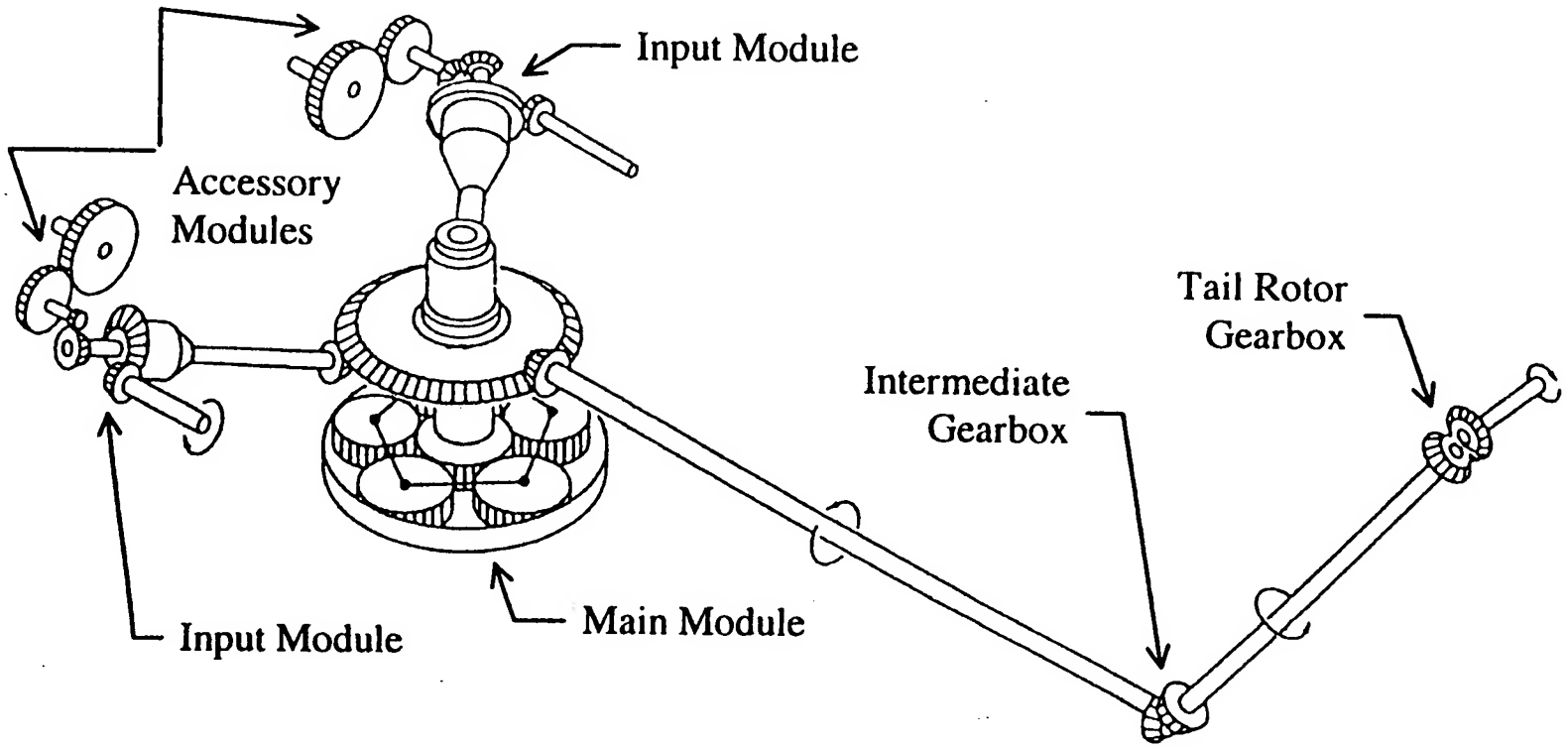

Figure 4.10: Seahawk drivetrain.

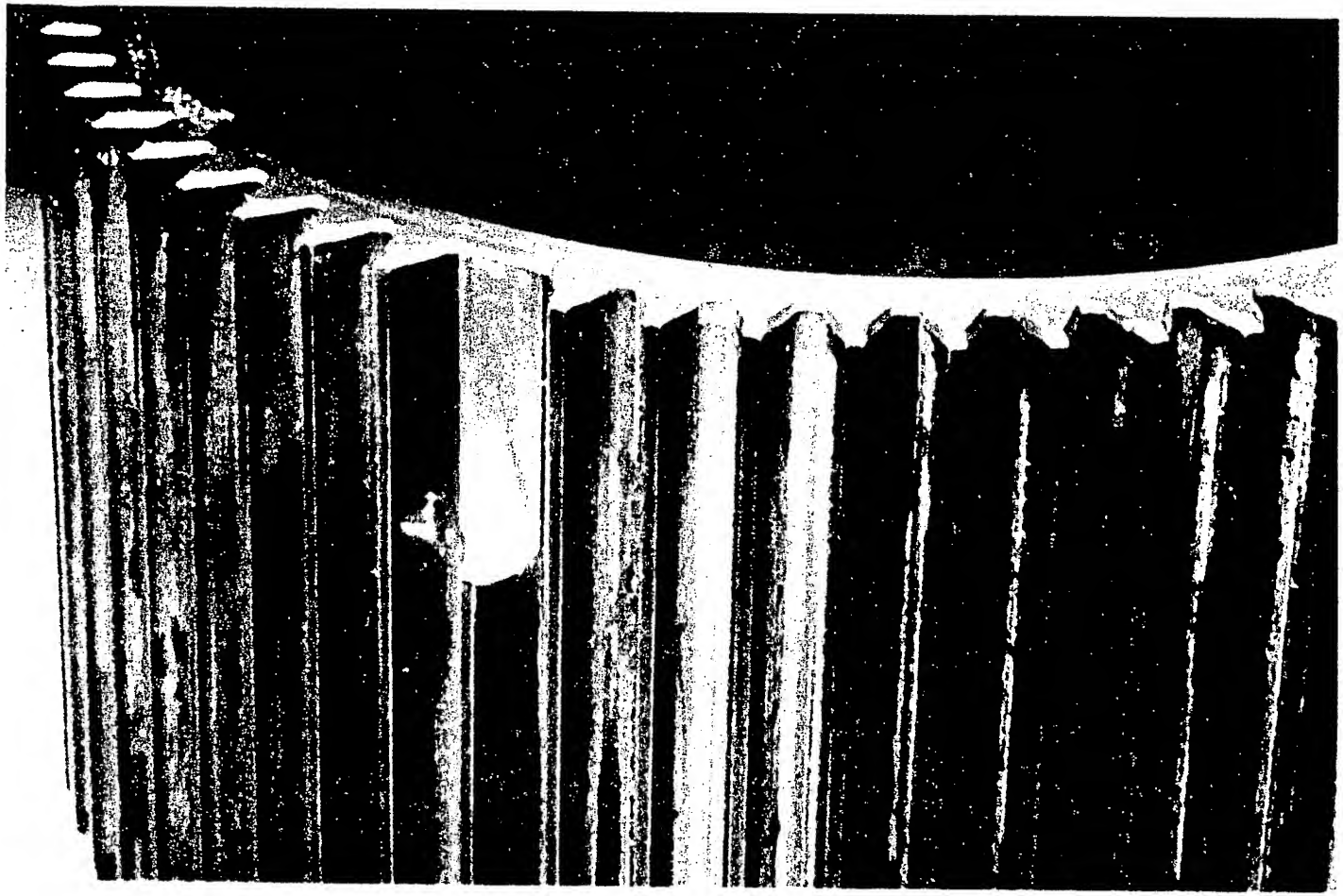

Figure 4.11 CH-60B sun gear with one third of a tooth removed.

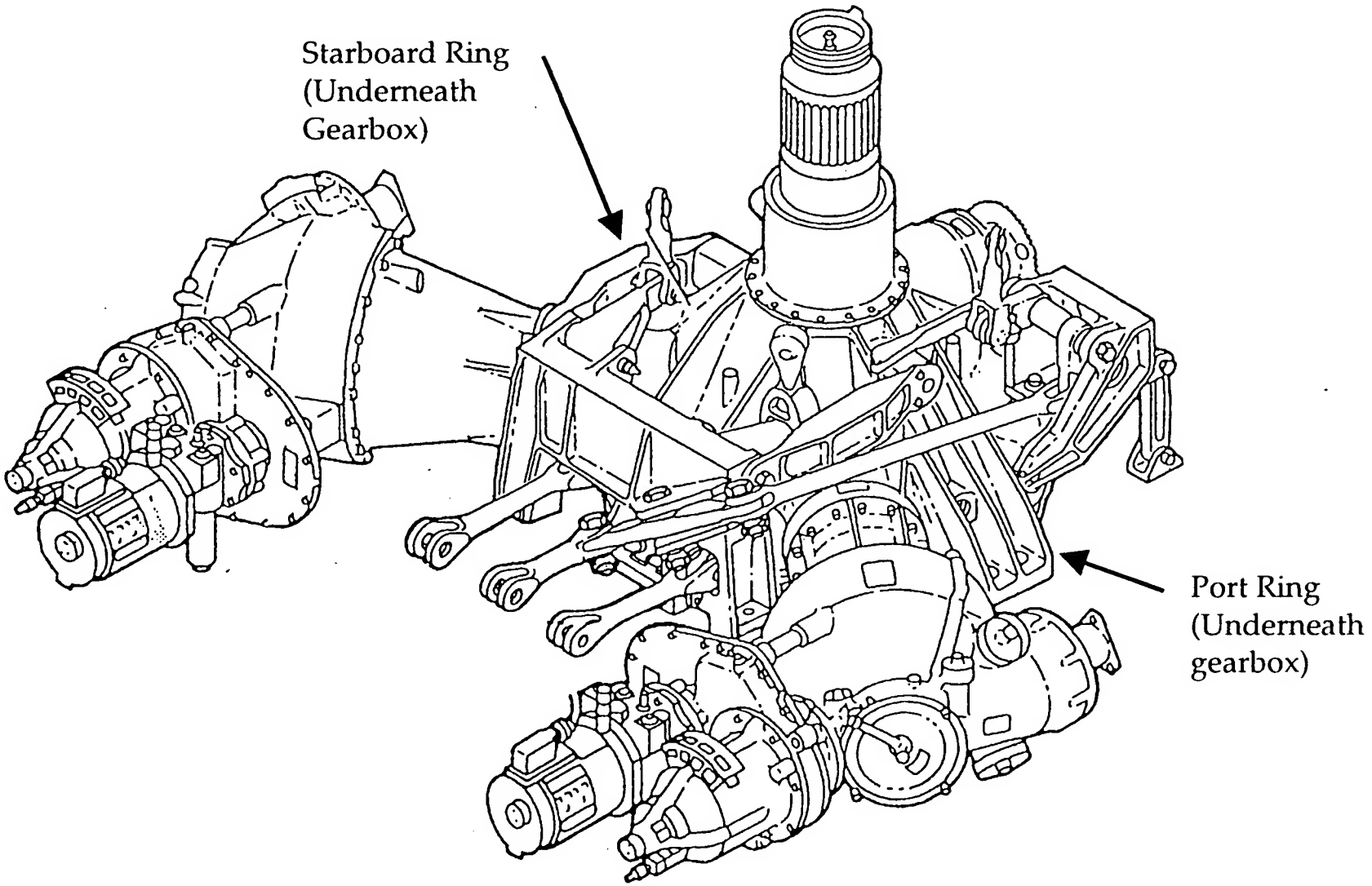

Figure 4.12: Seahawk transmission sensor locations.

a)

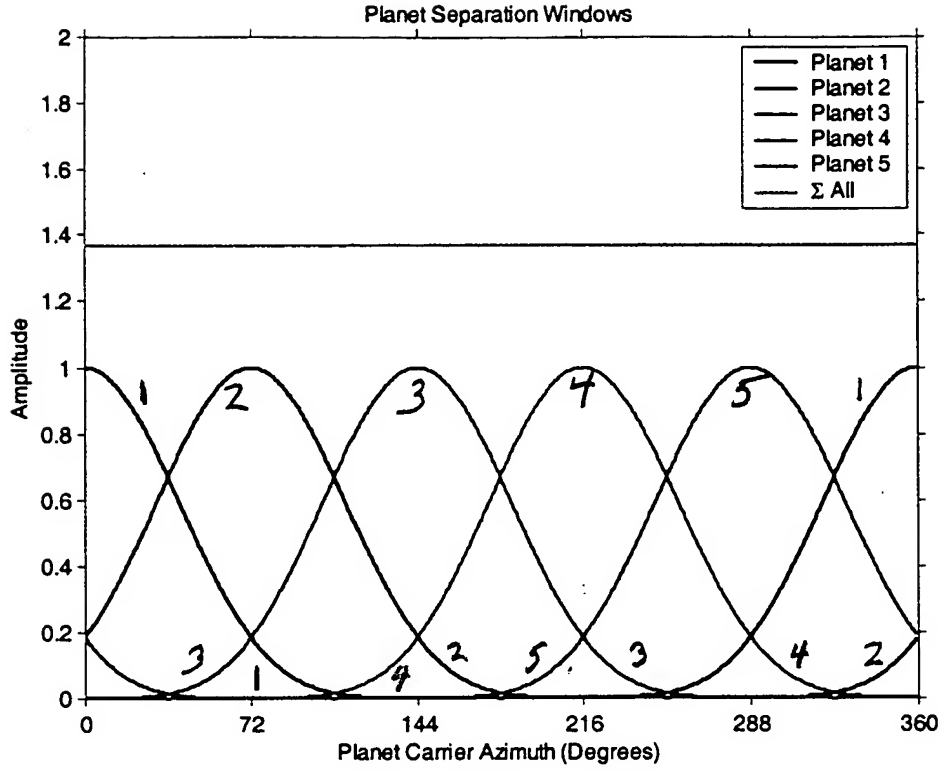

b)

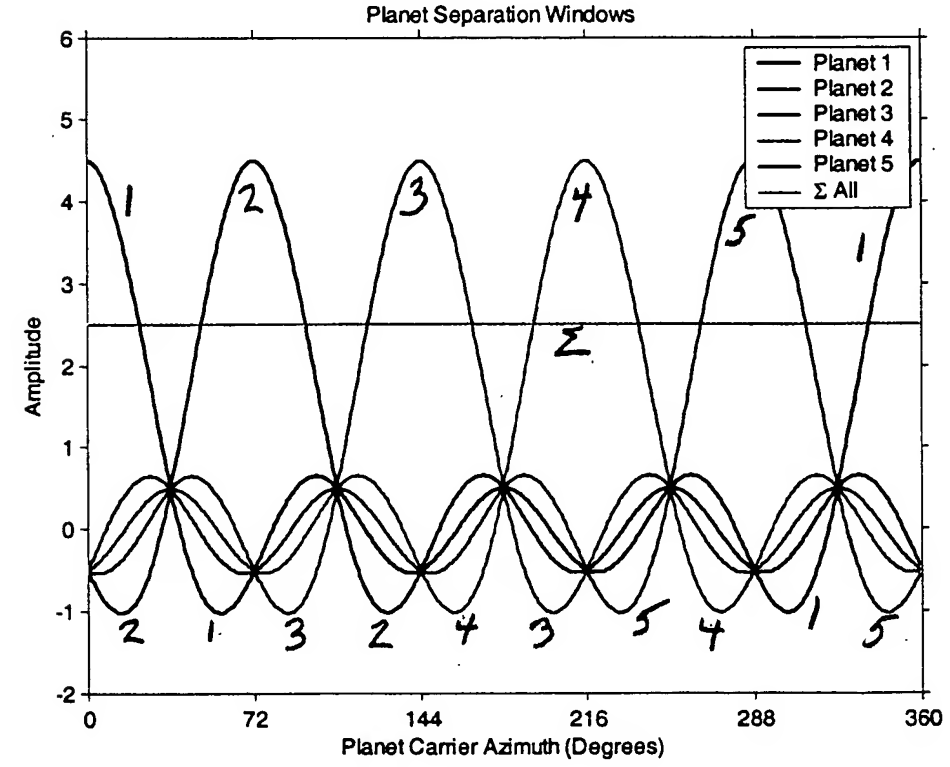

Figure 4.13: Planet separation windows for a five-planet gear train: a) $w_{power}(t)$, b) $w_{sum}(t)$.

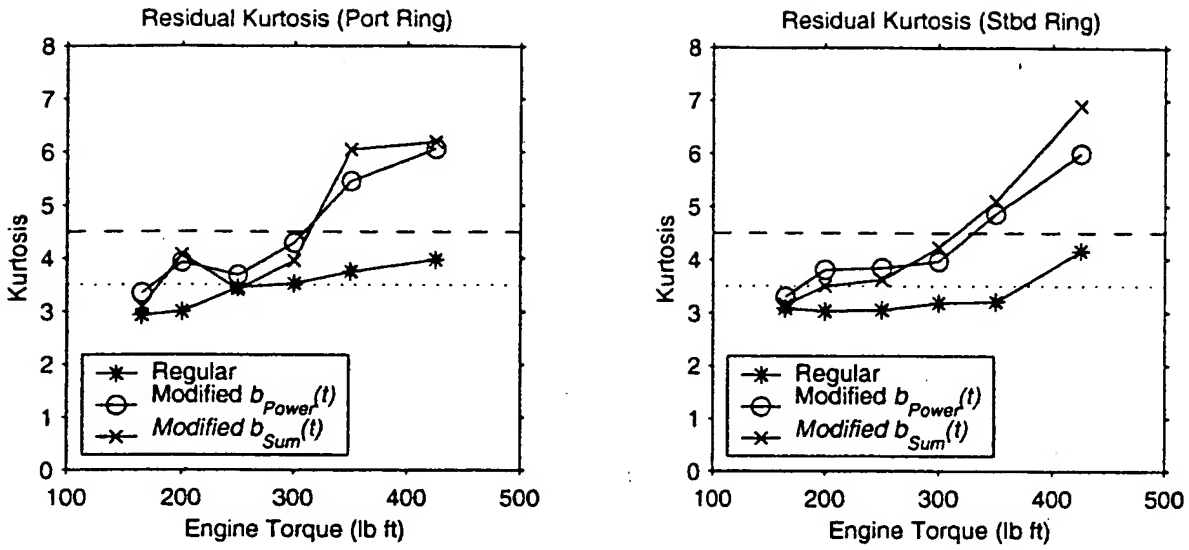

Figure 4.14: Residual signal kurtosis values.

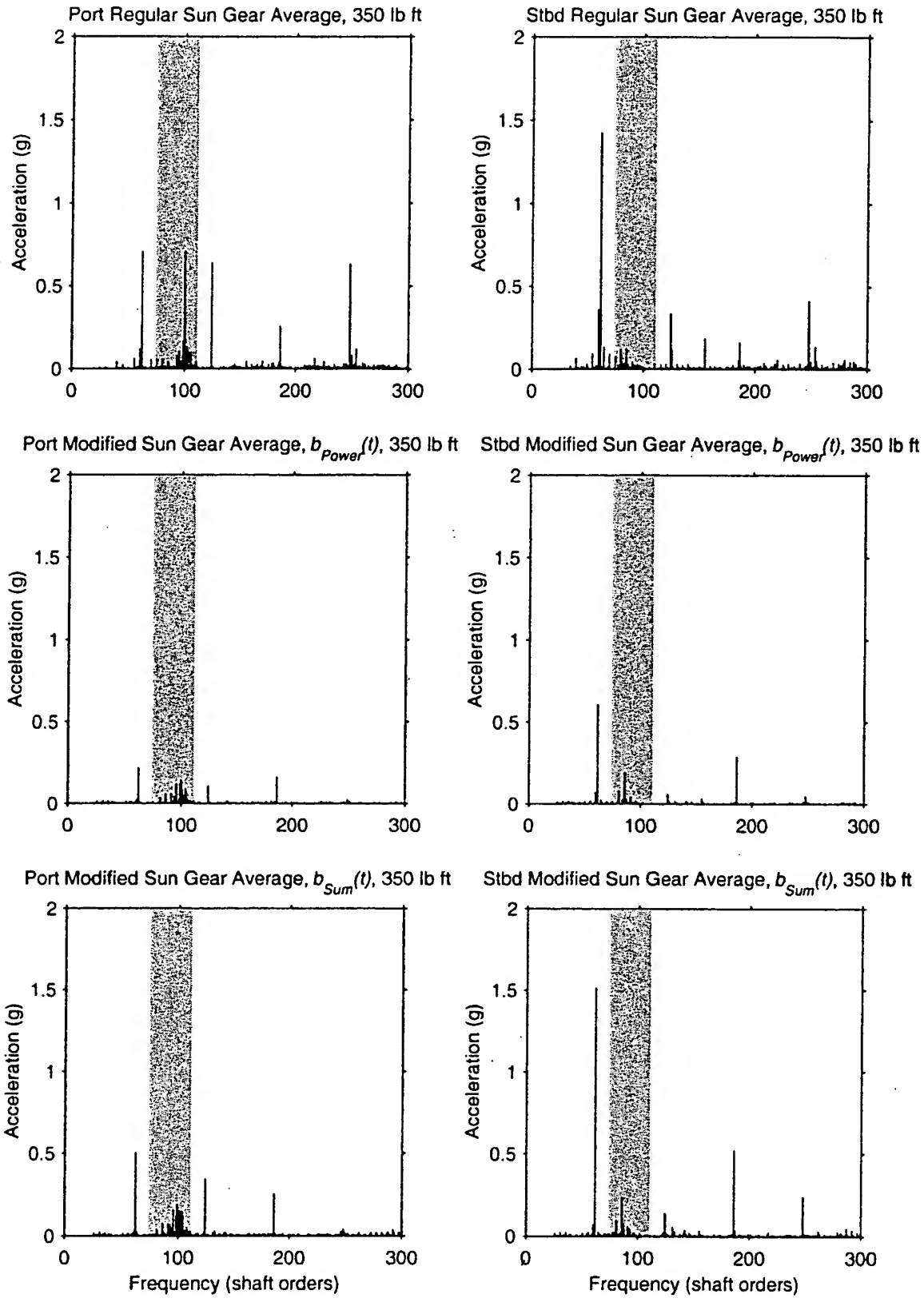

Figure 4.15: Spectra of sun gear averages at 350 lb ft torque showing resonance band.

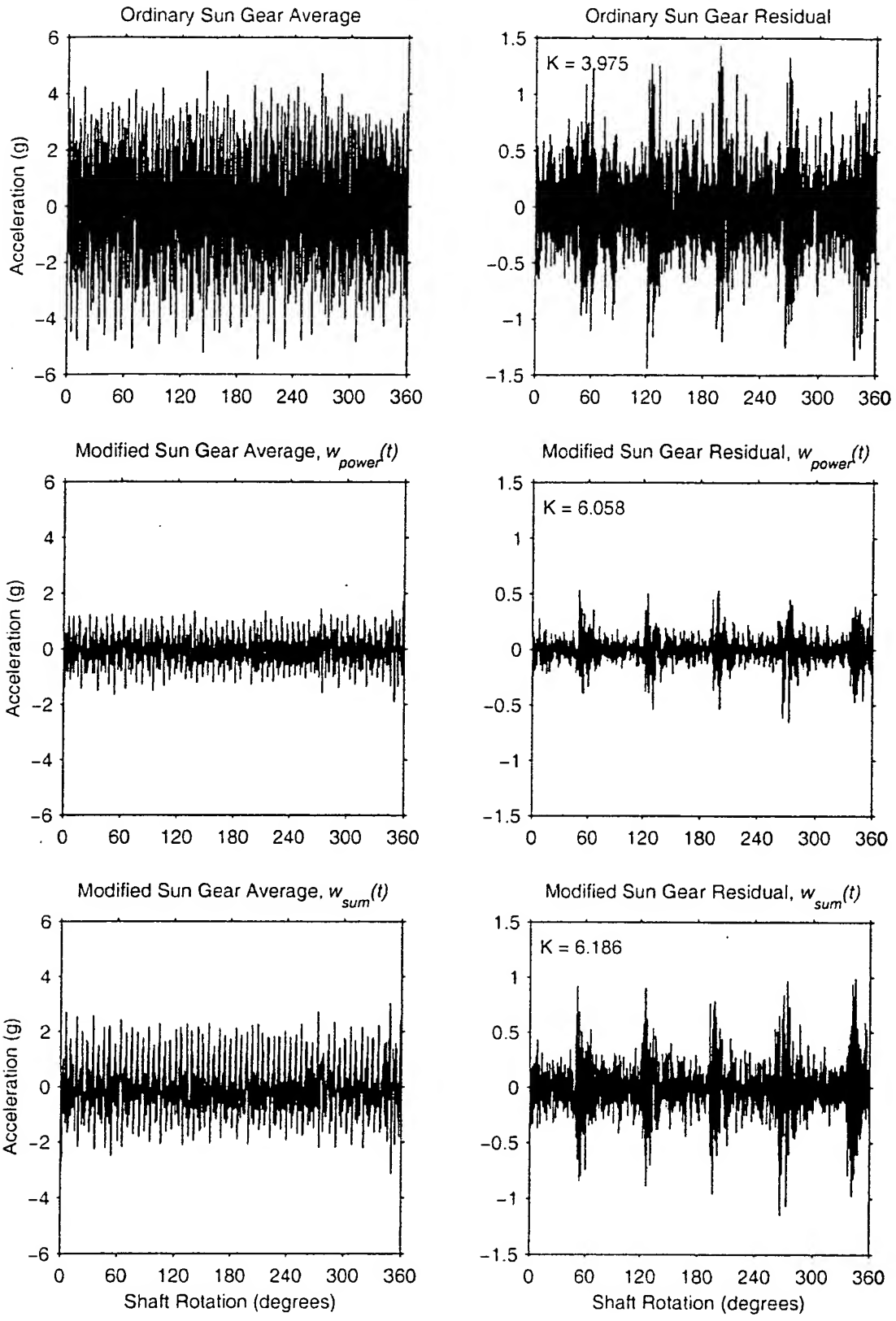

Figure 4.16: Sun gear averages, 425 lb ft torque, port ring accelerometer.

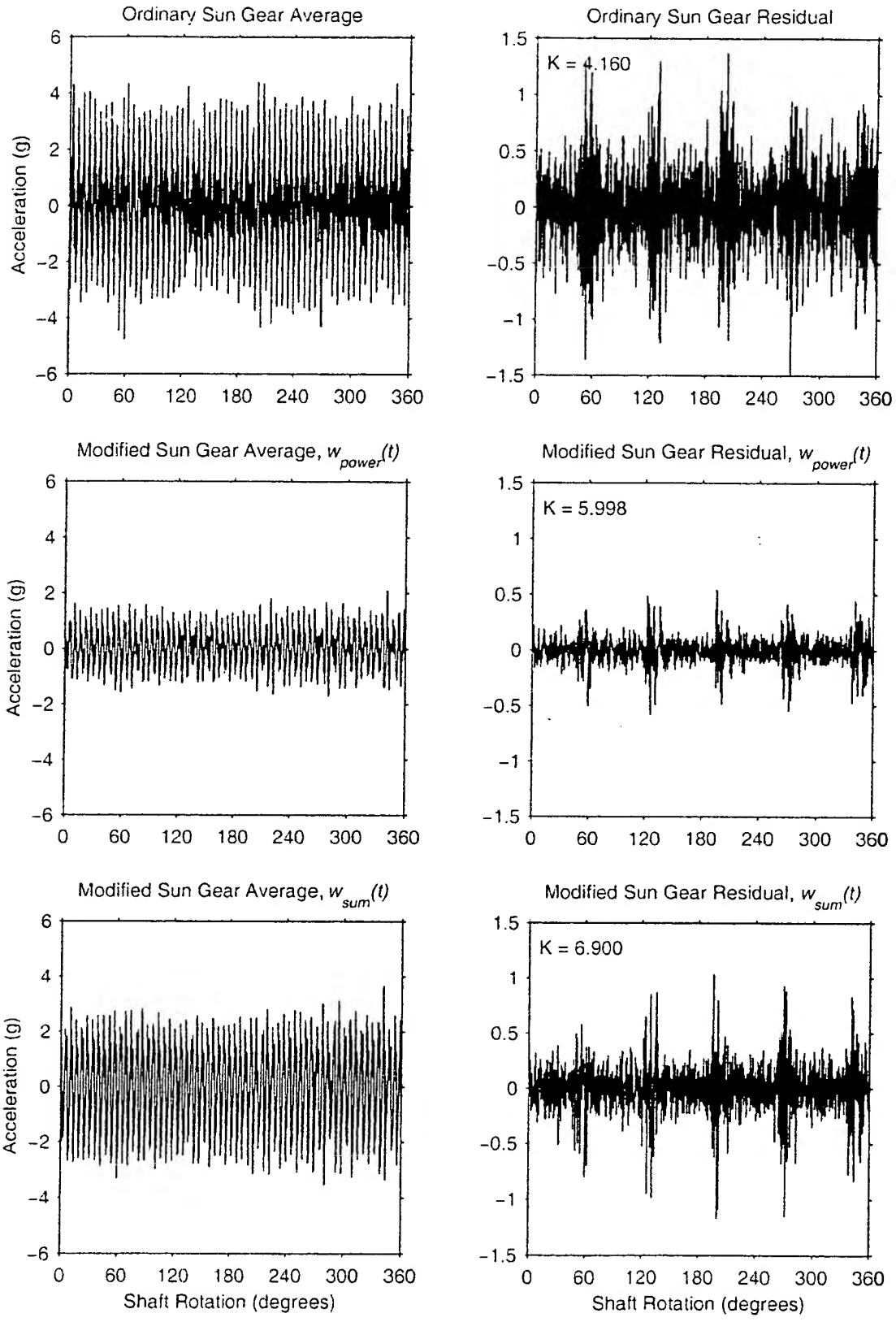

Figure 4.17: Sun gear averages, 425 lb ft torque, starboard ring accelerometer.

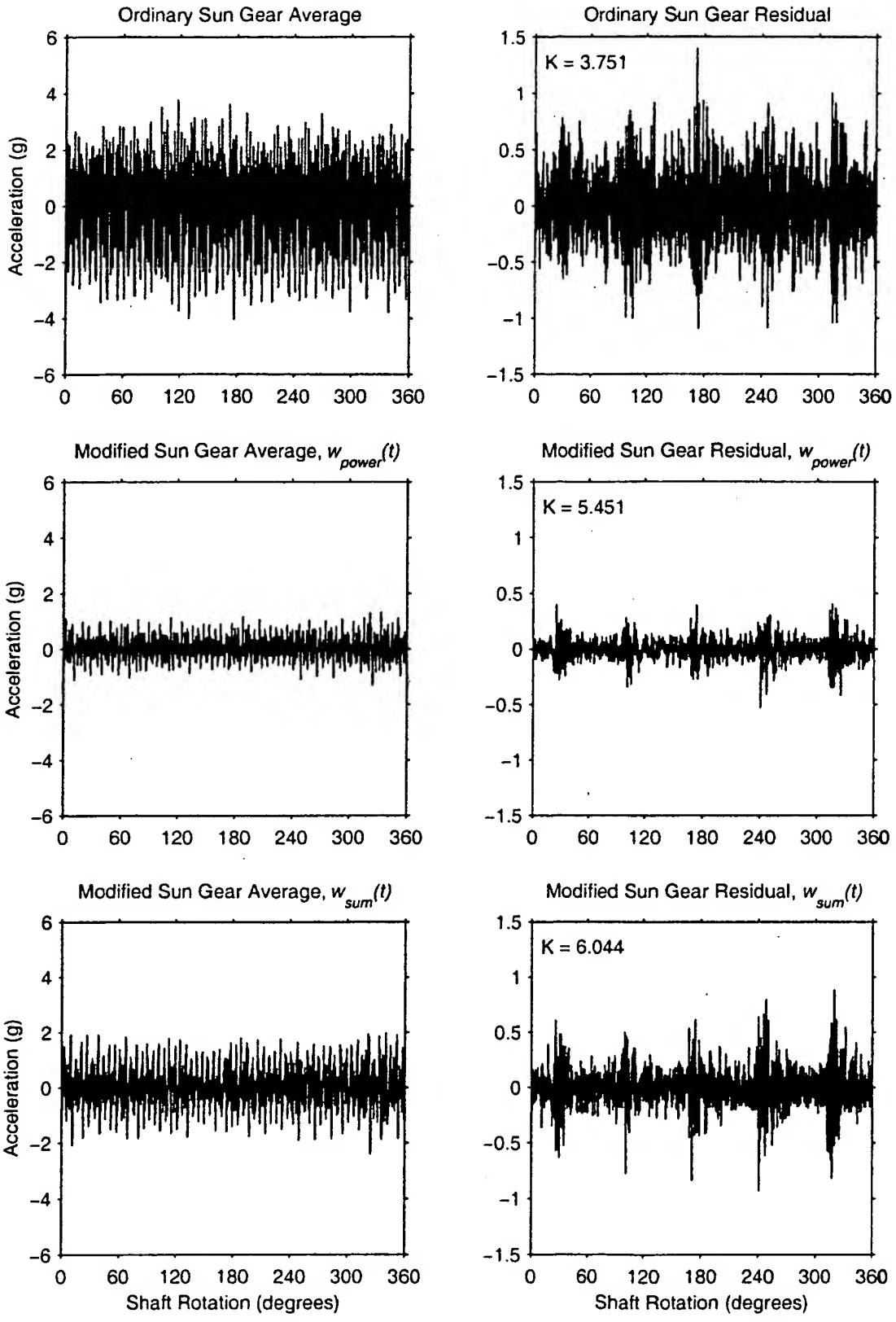

Figure 4.18: Sun gear averages, 350 lb ft torque, port ring accelerometer.

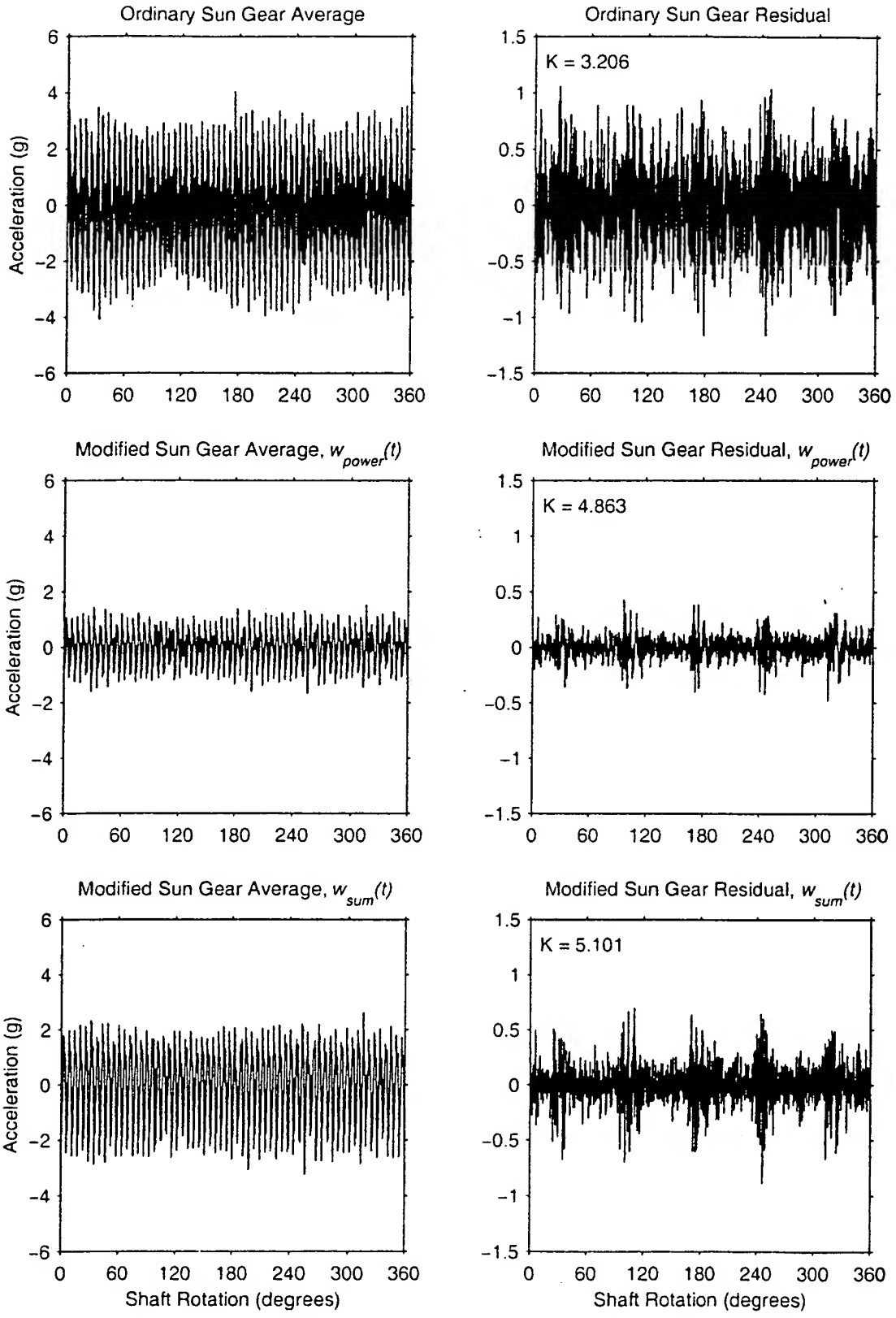

Figure 4.19: Sun gear averages, 350 lb ft torque, starboard ring accelerometer.

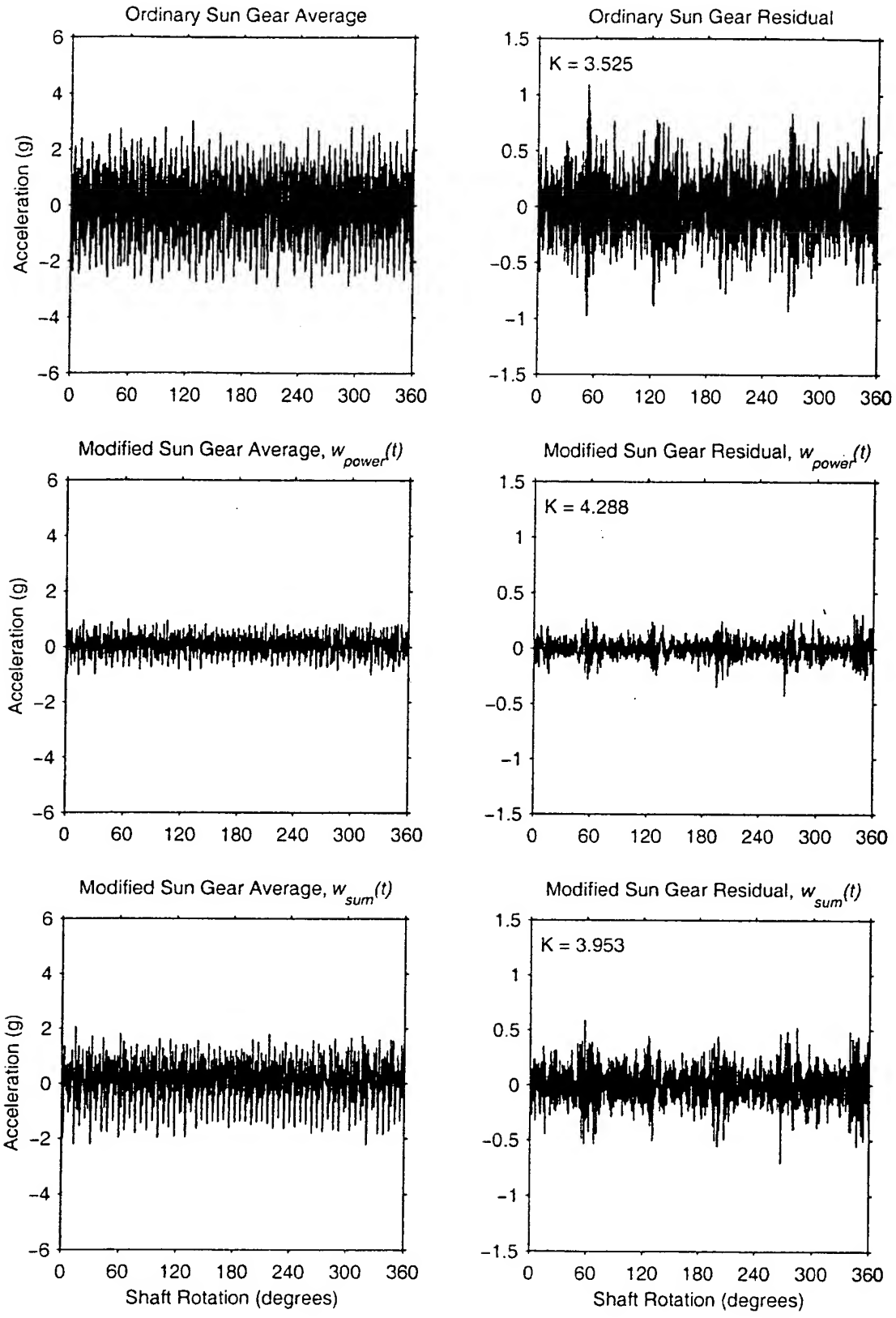

Figure 4.20: Sun gear averages, 300 lb ft torque, port ring accelerometer.

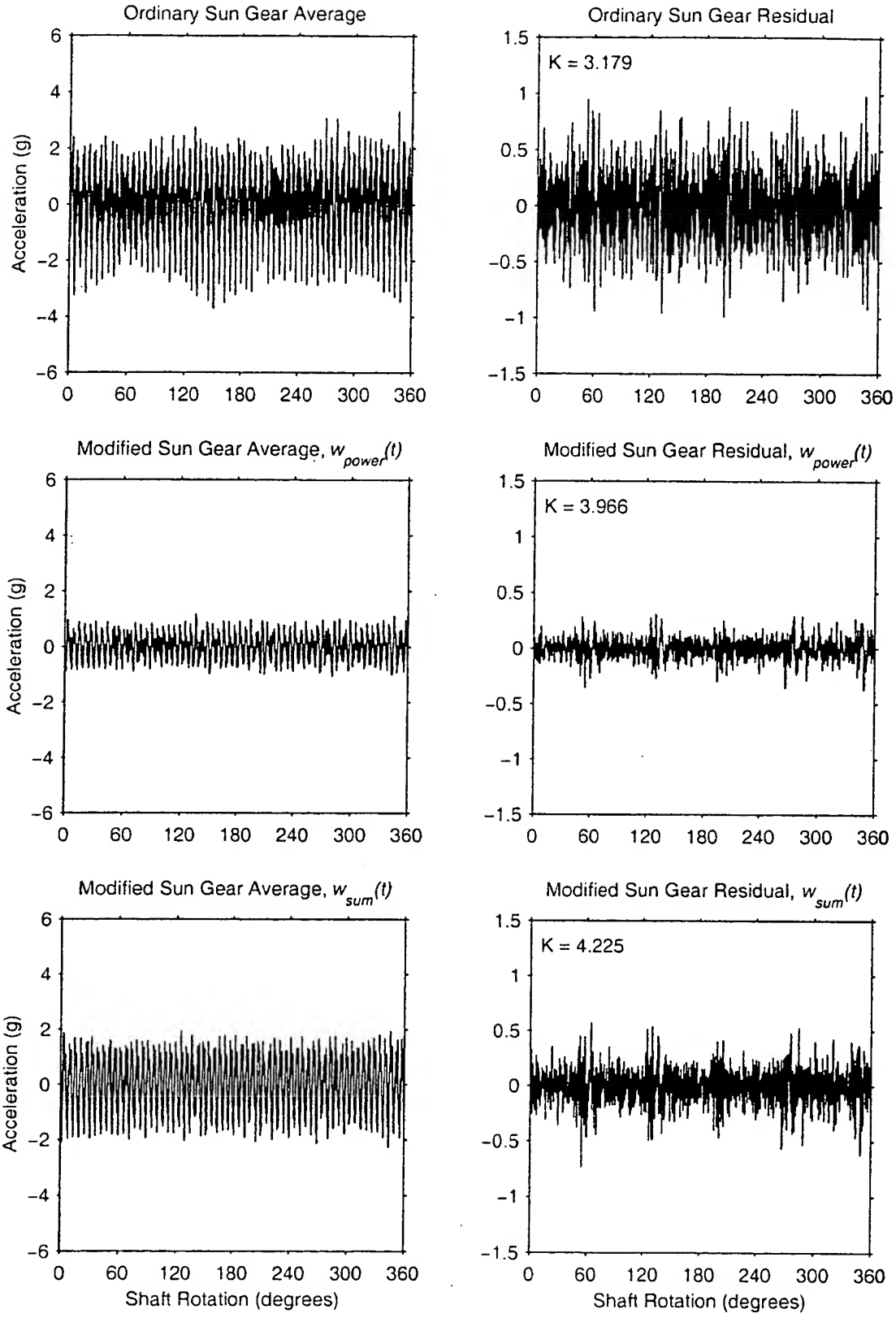

Figure 4.21: Sun gear averages, 300 lb ft torque, starboard ring accelerometer.

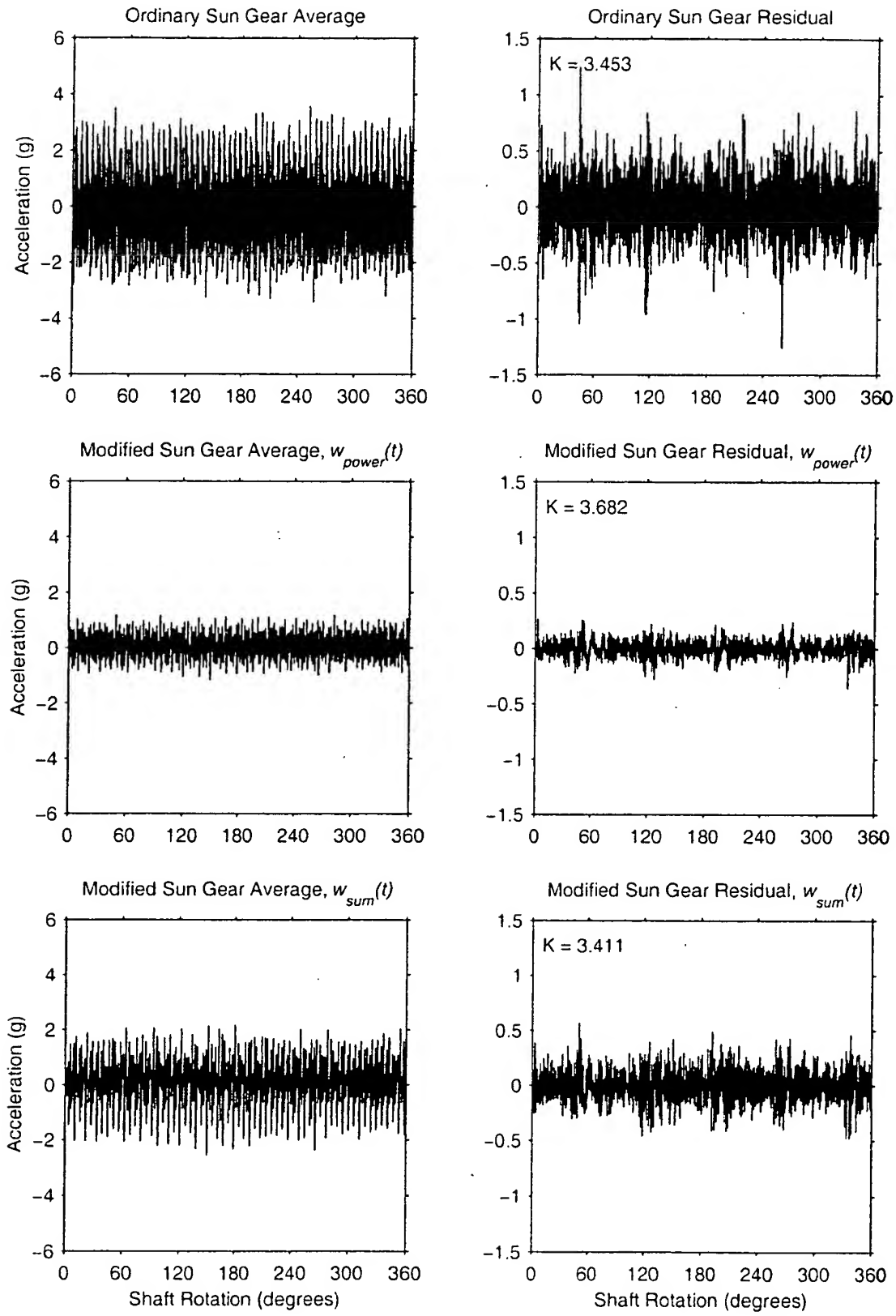

Figure 4.22: Sun gear averages, 250 lb ft torque, port ring accelerometer.

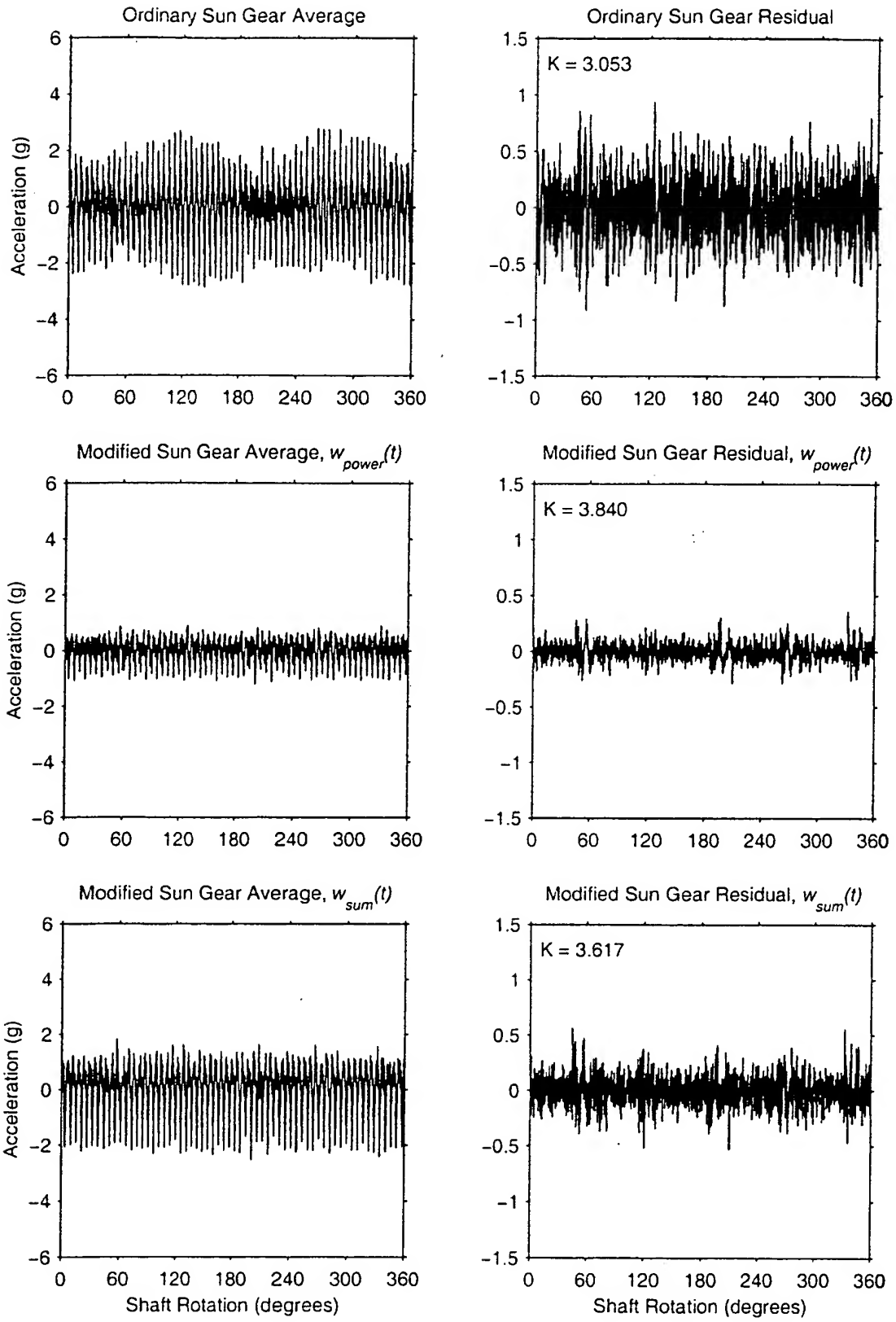

Figure 4.23: Sun gear averages, 250 lb ft torque, starboard ring accelerometer.

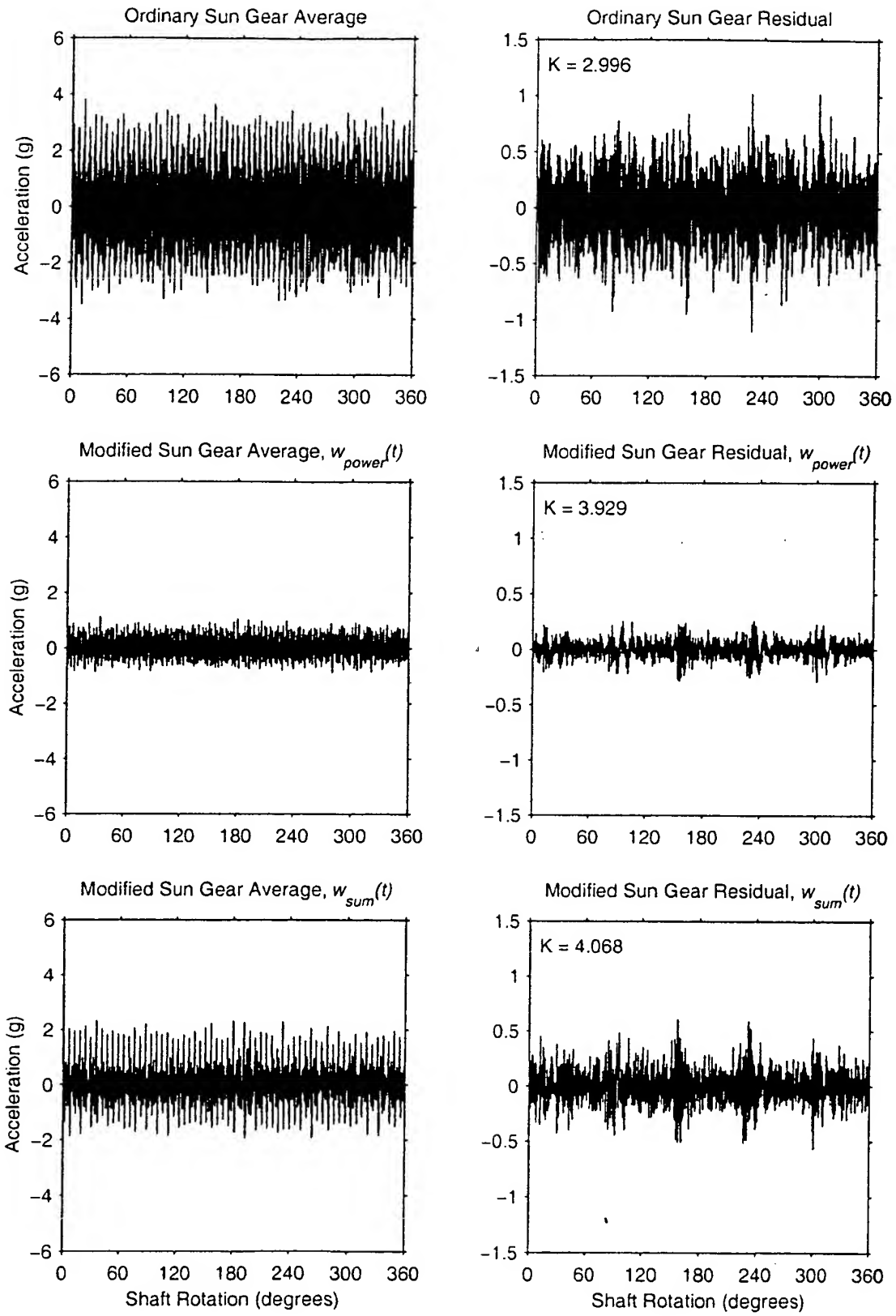

Figure 4.24: Sun gear averages, 200 lb ft torque, port ring accelerometer.

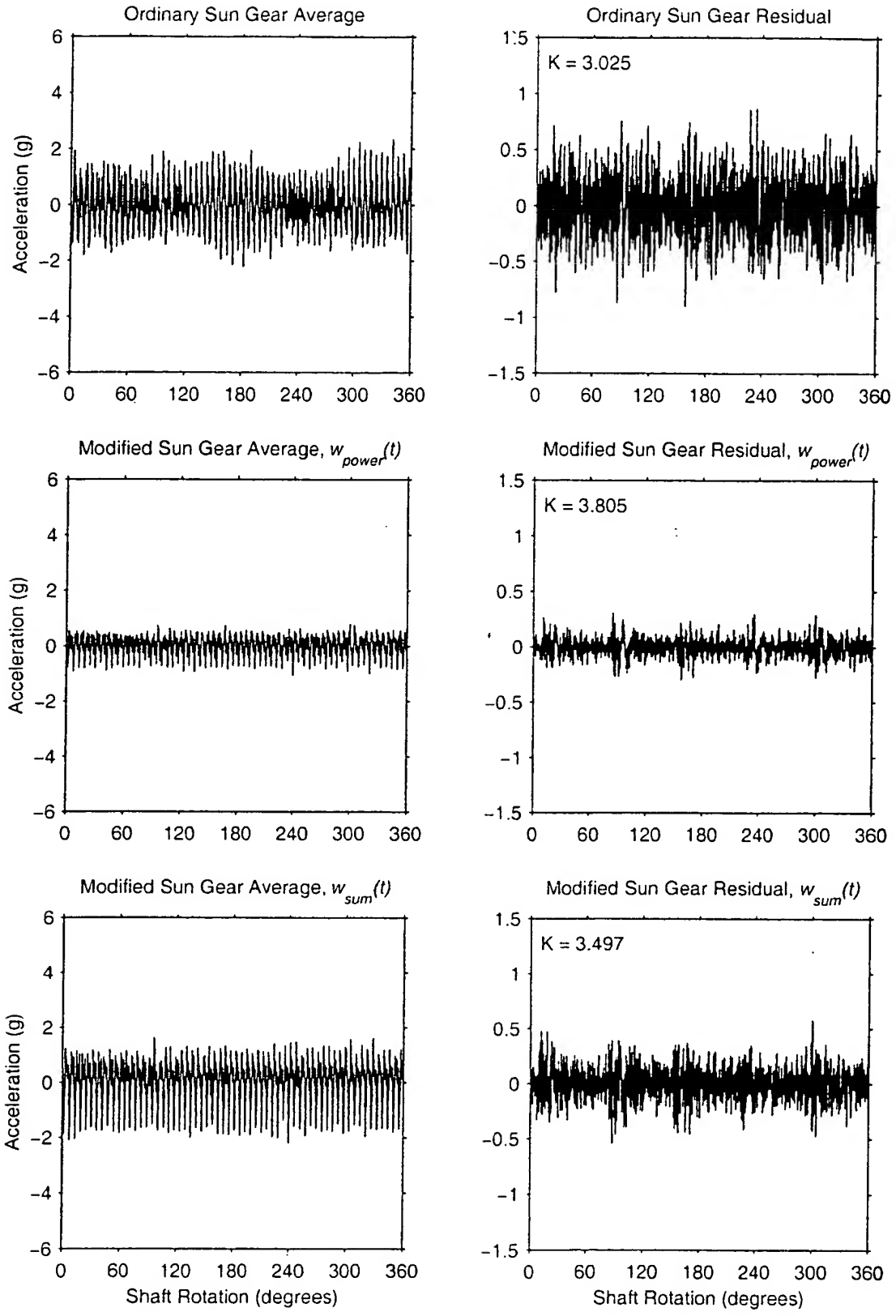

Figure 4.25: Sun gear averages, 200 lb ft torque, starboard ring accelerometer.

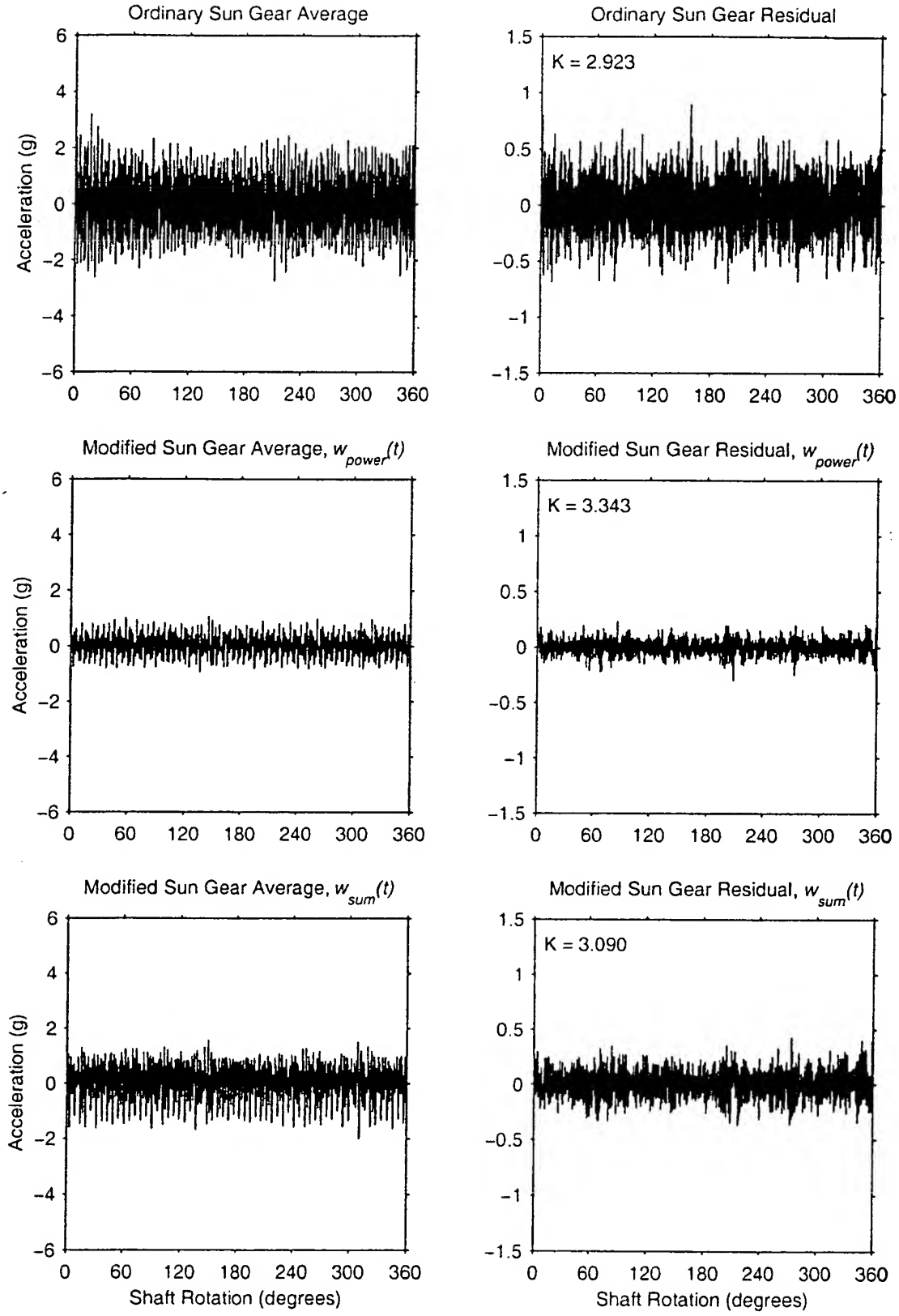

Figure 4.26: Sun gear averages, 165 lb ft torque, port ring accelerometer.

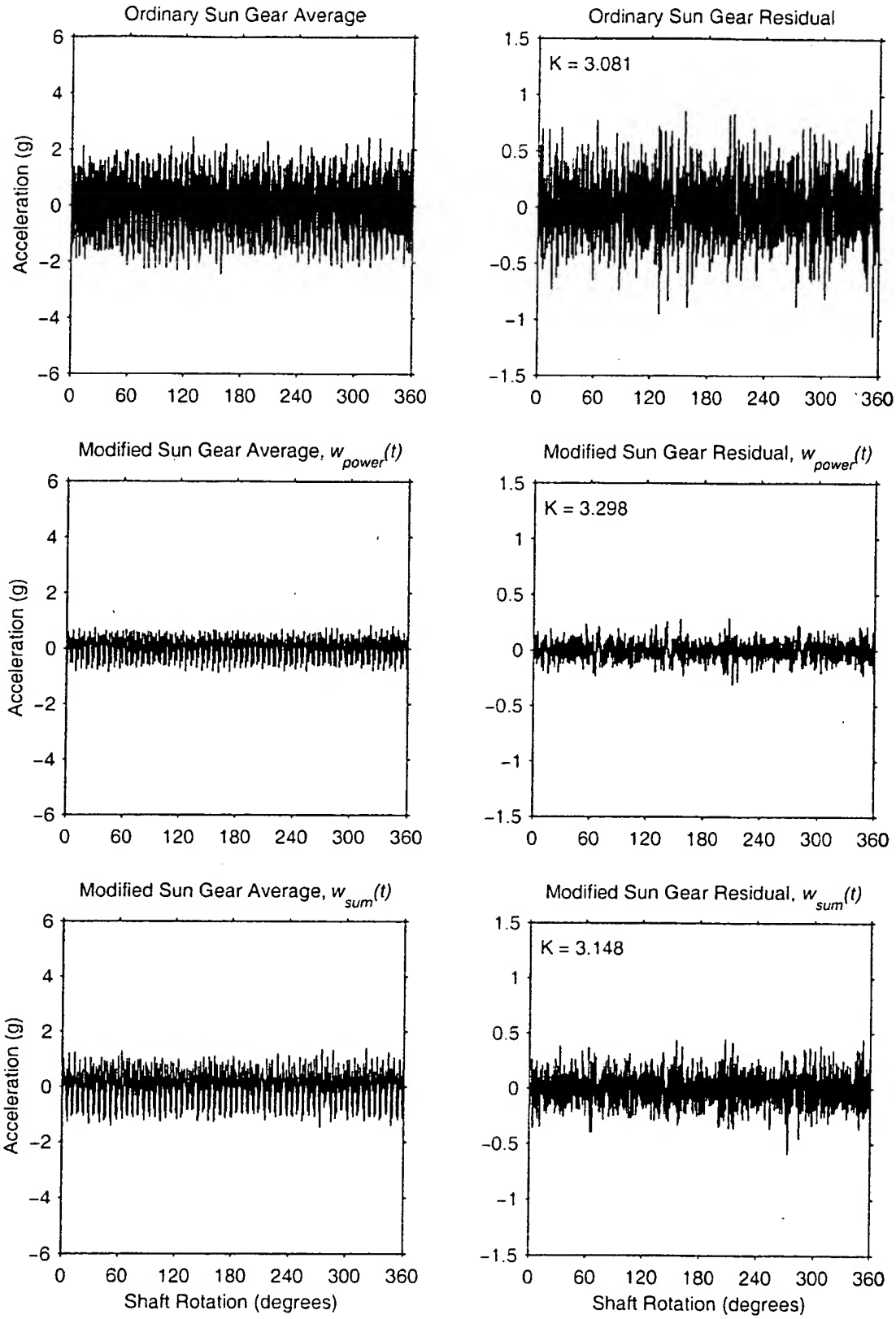

Figure 4.27: Sun gear averages, 165 lb ft torque, starboard ring accelerometer.

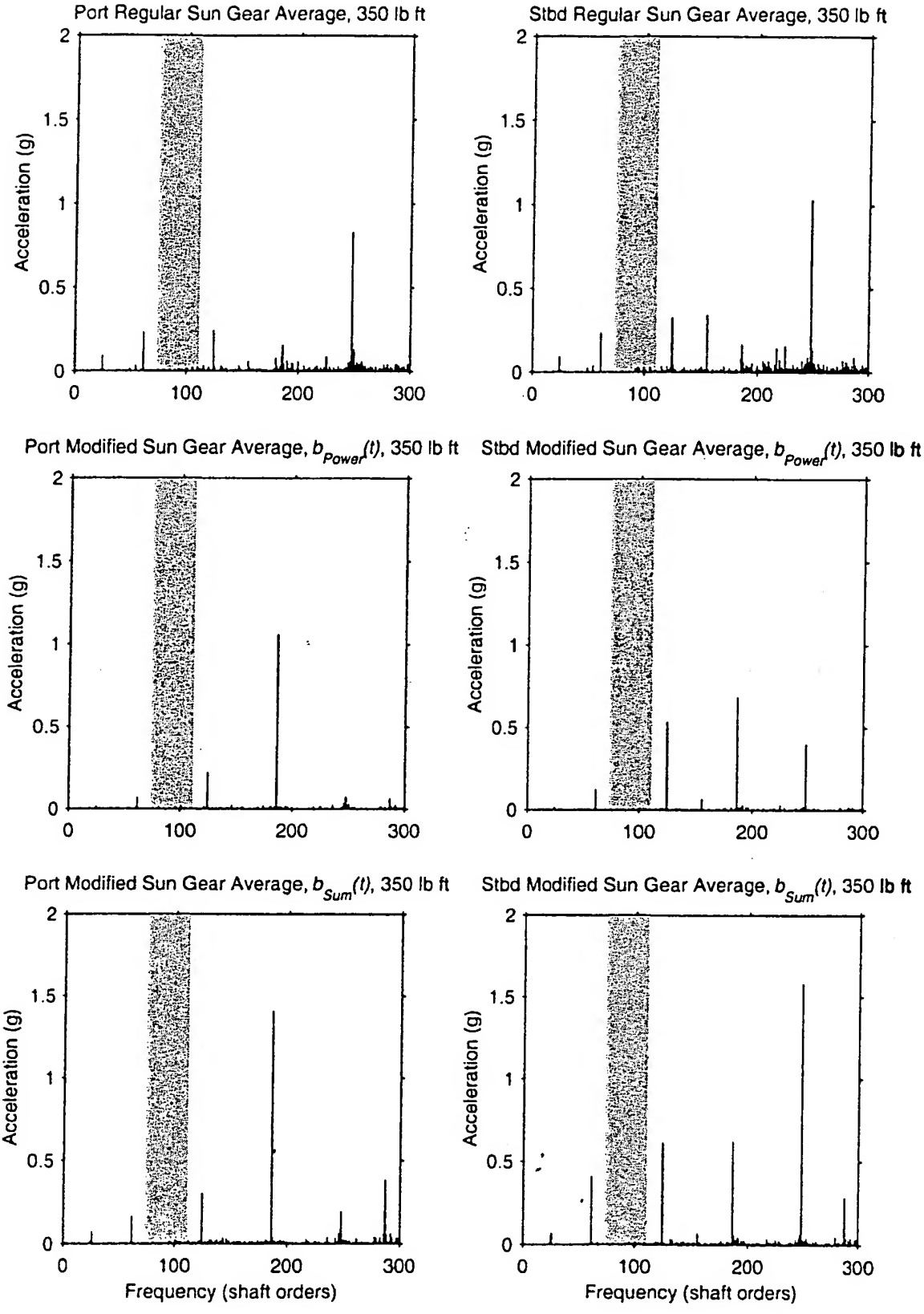

Figure 4.28: Spectra of sun gear averages at 350 lb ft from a gearbox without a sun gear fault.